ISSN 1948-5204 (online)

# World Journal of *Gastrointestinal Oncology*

*World J Gastrointest Oncol* 2022 February 15; 14(2): 369-546

Published by Baishideng Publishing Group Inc

World Journal of Gastrointestinal Oncology

Contents

Monthly Volume 14 Number 2 February 15, 2022

## EDITORIAL



## REVIEW



## MINIREVIEWS



## ORIGINAL ARTICLE

### Basic Study



### Clinical and Translational Research

*World Journal of Gastrointestinal Oncology*

**Monthly Volume 14 Number 2 February 15, 2022**

## Contents

*World Journal of Gastrointestinal Oncology*

**Monthly Volume 14 Number 2 February 15, 2022**

## Contents

## ABOUT COVER

Editorial Board Member of *World Journal of Gastrointestinal Oncology*, Filippo Lococo, MD, PhD, Assistant Professor, Department of Thoracic Surgery, Catholic University, Rome 00168, Italy. filippo_lococo@yahoo.it

## AIMS AND SCOPE

The primary aim of *World Journal of Gastrointestinal Oncology* (*WJGO*, *World J Gastrointest Oncol*) is to provide scholars and readers from various fields of gastrointestinal oncology with a platform to publish high-quality basic and clinical research articles and communicate their research findings online.

*WJGO* mainly publishes articles reporting research results and findings obtained in the field of gastrointestinal oncology and covering a wide range of topics including liver cell adenoma, gastric neoplasms, appendiceal neoplasms, biliary tract neoplasms, hepatocellular carcinoma, pancreatic carcinoma, cecal neoplasms, colonic neoplasms, colorectal neoplasms, duodenal neoplasms, esophageal neoplasms, gallbladder neoplasms, *etc*.

## INDEXING/ABSTRACTING

The *WJGO* is now indexed in Science Citation Index Expanded (also known as SciSearch®), PubMed, PubMed Central, and Scopus. The 2021 edition of Journal Citation Reports® cites the 2020 impact factor (IF) for *WJGO* as 3.393; IF without journal self cites: 3.333; 5-year IF: 3.519; Journal Citation Indicator: 0.5; Ranking: 163 among 242 journals in oncology; Quartile category: Q3; Ranking: 60 among 92 journals in gastroenterology and hepatology; and Quartile category: Q3. The *WJGO*'s CiteScore for 2020 is 3.3 and Scopus CiteScore rank 2020: Gastroenterology is 70/136.

## RESPONSIBLE EDITORS FOR THIS ISSUE

**Production Editor:** *Ying-Yi Yuan*; **Production Department Director:** *Xiang Li*; **Editorial Office Director:** *Ya-Juan Ma.*

**NAME OF JOURNAL**
*World Journal of Gastrointestinal Oncology*

**ISSN**
ISSN 1948-5204 (online)

**LAUNCH DATE**
February 15, 2009

**FREQUENCY**
Monthly

**EDITORS-IN-CHIEF**
Monjur Ahmed, Florin Burada

**EDITORIAL BOARD MEMBERS**
https://www.wjgnet.com/1948-5204/editorialboard.htm

**PUBLICATION DATE**
February 15, 2022



**INSTRUCTIONS TO AUTHORS**
https://www.wjgnet.com/bpg/gerinfo/204

**GUIDELINES FOR ETHICS DOCUMENTS**
https://www.wjgnet.com/bpg/GerInfo/287

**GUIDELINES FOR NON-NATIVE SPEAKERS OF ENGLISH**
https://www.wjgnet.com/bpg/gerinfo/240

**PUBLICATION ETHICS**
https://www.wjgnet.com/bpg/GerInfo/288

**PUBLICATION MISCONDUCT**
https://www.wjgnet.com/bpg/gerinfo/208

**ARTICLE PROCESSING CHARGE**
https://www.wjgnet.com/bpg/gerinfo/242

**STEPS FOR SUBMITTING MANUSCRIPTS**
https://www.wjgnet.com/bpg/GerInfo/239

**ONLINE SUBMISSION**
https://www.f6publishing.com

World Journal of Gastrointestinal Oncology

Submit a Manuscript: https://www.f6publishing.com

*World J Gastrointest Oncol* 2022 February 15; 14(2): 450-477

DOI: 10.4251/wjgo.v14.i2.450

ISSN 1948-5204 (online)

ORIGINAL ARTICLE

Basic Study

# Frankincense myrrh attenuates hepatocellular carcinoma by regulating tumor blood vessel development through multiple epidermal growth factor receptor-mediated signaling pathways

Piao Zheng, Zhen Huang, Dong-Chang Tong, Qing Zhou, Sha Tian, Bo-Wei Chen, Di-Min Ning, Yin-Mei Guo, Wen-Hao Zhu, Yan Long, Wei Xiao, Zhe Deng, Yi-Chen Lei, Xue-Fei Tian

**ORCID number:** Piao Zheng 0000-0003-3649-8181; Zhen Huang 0000-0002-8437-7141; Dong-Chang Tong 0000-0003-0030-2837; Qing Zhou 0000-0002-9633-7542; Sha Tian 0000-0002-2557-5674; Bo-Wei Chen 0000-0001-8835-7829; Di-Min Ning 0000-0003-4335-7141; Yin-Mei Guo 0000-0003-0635-1218; Wen-Hao Zhu 0000-0002-2326-7475; Yan Long 0000-0002-4894-1489; Wei Xiao 0000-0002-9258-591X; Zhe Deng 0000-0002-3283-6289; Yi-Chen Lei 0000-0002-5791-2161; Xue-Fei Tian 0000-0003-4786-0844.

**Author contributions:** Tian XF provided the conceptual and technical guidance, designed the study, and revised the manuscript critically for important intellectual content; Zheng P, Tian S and Zhou Q coordinated the study; Zheng P, Huang Z, Tong DC, Ning DM, Guo YM, Zhu WH, Long Y, Deng Z and Lei YC performed the experiments; Zheng P, Chen BW and Xiao W interpreted data; Zheng P wrote the manuscript; all authors approved the final version of the article.

**Institutional animal care and use committee statement:** This research was reviewed and approved by the Committee on the Ethics of Animal

**Piao Zheng, Zhen Huang, Dong-Chang Tong, Sha Tian, Di-Min Ning, Wen-Hao Zhu, Zhe Deng, Yi-Chen Lei, Xue-Fei Tian,** College of Integrated Traditional Chinese and Western Medicine, Hunan University of Chinese Medicine, Changsha 410208, Hunan Province, China

**Piao Zheng,** Department of Integrated Traditional Chinese and Western Medicine, The Second Xiangya Hospital, Central South University, Changsha 410011, Hunan Province, China

**Qing Zhou, Bo-Wei Chen, Yan Long,** The First Affiliated Hospital, Hunan University of Chinese Medicine, Changsha 410021, Hunan Province, China

**Yin-Mei Guo,** Hunan Key Laboratory of Translational Research in Formulas and Zheng of Traditional Chinese Medicine, Hunan University of Chinese Medicine, Changsha 410208, Hunan Province, China

**Wei Xiao,** Institute of Integrative Medicine, Department of Integrated Traditional Chinese and Western Medicine, Xiangya Hospital, Central South University, Changsha 410008, Hunan Province, China

**Corresponding author:** Xue-Fei Tian, PhD, Professor, College of Integrated Traditional Chinese and Western Medicine, Hunan University of Chinese Medicine, No. 300 Xueshi Road, Yuelu District, Changsha 410208, Hunan Province, China. 003640@hnucm.edu.cn

## Abstract

### *BACKGROUND*

In traditional Chinese medicine (TCM), frankincense and myrrh are the main components of the antitumor drug Xihuang Pill. These compounds show anticancer activity in other biological systems. However, whether frankincense and/or myrrh can inhibit the occurrence of hepatocellular carcinoma (HCC) is unknown, and the potential molecular mechanism(s) has not yet been determined.

### *AIM*

To predict and determine latent anti-HCC therapeutic targets and molecular mechanisms of frankincense and myrrh *in vivo*.

Experiments of Hunan University of Chinese Medicine, No. LL2020102801. All animal experiments were conducted in accordance with international standards and under the guidelines for animal care and use formulated by the Animal Experiment Center of Hunan University of Chinese Medicine.

**Conflict-of-interest statement:** All authors declare no financial or commercial conflict of interest.

**Data sharing statement:** All data generated or analyzed during this study are included in this published article.

**ARRIVE guidelines statement:** The authors have read the ARRIVE guidelines, and the manuscript was prepared and revised according to the ARRIVE guidelines.

**Supported by** the National Natural Science Foundation of China, No. U20A20408 (Major Program) and No. 82074450 (General Program); Natural Science Foundation of Hunan Province, No. 2020JJ4066; Hunan Province Research and innovation projects for Postgraduates, No. CX20190541; Hunan Province "domestic first-class cultivation discipline" Integrated Traditional Chinese and Western medicine open fund project, No. 2018ZXYJH03; Hunan University Undergraduate Research Learning and Innovative Experiment Project, No. 201609030114.

**Country/Territory of origin:** China

**Specialty type:** Oncology

**Provenance and peer review:** Unsolicited article; Externally peer reviewed.

**Peer-review model:** Single blind

**Peer-review report's scientific quality classification**

Grade A (Excellent): 0
Grade B (Very good): B
Grade C (Good): 0
Grade D (Fair): 0
Grade E (Poor): 0

***METHODS***

In the present study, which was based on the Traditional Chinese Medicine Systems Pharmacology Database and Analysis Platform (http://tcmspw.com/tcmsp.php), Universal Protein database (http://www.uniprot.org), GeneCards: The Human Gene Database (http://www.genecards.org/) and Comparative Toxicogenomics Database (http://www.ctdbase.org/), the efficacy of and mechanism by which frankincense and myrrh act as anti-HCC compounds were predicted. The core prediction targets were screened by molecular docking. *In vivo*, SMMC-7721 human liver cancer cells were transplanted as xenografts into nude mice to establish a subcutaneous tumor model, and two doses of frankincense plus myrrh or one dose of an EGFR inhibitor was administered to these mice continuously for 14 d. The tumors were collected and evaluated: the tumor volume and growth rate were gauged to evaluate tumor growth; hematoxylin-eosin staining was performed to estimate histopathological changes; immunofluorescence (IF) was performed to detect the expression of CD31, α-SMA and collagen IV; transmission electron microscopy (TEM) was conducted to observe the morphological structure of vascular cells; enzyme-linked immunosorbent assay (ELISA) was performed to measure the levels of secreted HIF-1α and TNF-α; reverse transcription-polymerase chain reaction (RT-qPCR) was performed to measure the mRNA expression of HIF-1α, TNF-α, VEGF and MMP-9; and Western blot (WB) was performed to determine the levels of proteins expressed in the EGFR-mediated PI3K/Akt and MAPK signaling pathways.

***RESULTS***

The results of the network pharmacology analysis showed that there were 35 active components in the frankincense and myrrh extracts targeting 151 key targets. The molecular docking analysis showed that both boswellic acid and stigmasterol showed strong affinity for the targets, with the greatest affinity for EGFR. Frankincense and myrrh treatment may play a role in the treatment of HCC by regulating hypoxia responses and vascular system-related pathological processes, such as cytokine-receptor binding, and pathways, such as those involving serine/threonine protein kinase complexes and MAPK, HIF-1 and ErbB signaling cascades. The animal experiment results were verified. First, we found that, through frankincense and/or myrrh treatment, the volume of subcutaneously transplanted HCC tumors was significantly reduced, and the pathological morphology was attenuated. Then, IF and TEM showed that frankincense and/or myrrh treatment reduced CD31 and collagen IV expression, increased the coverage of perivascular cells, tightened the connection between cells, and improved the shape of blood vessels. In addition, ELISA, RT-qPCR and WB analyses showed that frankincense and/or myrrh treatment inhibited the levels of hypoxia-inducible factors, inflammatory factors and angiogenesis-related factors, namely, HIF-1α, TNF-α, VEGF and MMP-9. Furthermore, mechanistic experiments illustrated that the effect of frankincense plus myrrh treatment was similar to that of an EGFR inhibitor with regard to controlling EGFR activation, thereby inhibiting the phosphorylation activity of its downstream targets: the PI3K/Akt and MAPK (ERK, p38 and JNK) pathways.

***CONCLUSION***

In summary, frankincense and myrrh treatment targets tumor blood vessels to exert anti-HCC effects *via* EGFR-activated PI3K/Akt and MAPK signaling pathways, highlighting the potential of this dual TCM compound as an anti-HCC candidate.

**Key Words:** Hepatocellular carcinoma; Frankincense; Myrrh; Network pharmacology; Tumor blood vessels; Multiple signaling pathways



**Core Tip:** Hepatocellular carcinoma (HCC) is a serious threat to human health, and its

**Received:** July 22, 2021
**Peer-review started:** July 22, 2021
**First decision:** November 8, 2021
**Revised:** November 19, 2021
**Accepted:** January 14, 2022
**Article in press:** January 14, 2022
**Published online:** February 15, 2022

**P-Reviewer:** Gupta T
**S-Editor:** Zhang H
**L-Editor:** A
**P-Editor:** Li JH

pathological process is closely related to blood vessels. Currently, powerful targeted drugs for HCC treatment are lacking. The discovery of new drugs is an urgent task. As a complementary and alternative therapy, traditional Chinese medicine has played an increasingly prominent role. This study introduces frankincense and myrrh derived from the classic anticancer Chinese patent medicine Xihuang Pill. Through prediction and verification, the findings confirmed that this frankincense and myrrh treatment targets tumor blood vessels through EGFR-activated PI3K/Akt and MAPK signaling pathways to exert anti-HCC effects. Frankincense and/or myrrh treatment might be a potential anti-HCC drug candidate.

**Citation:** Zheng P, Huang Z, Tong DC, Zhou Q, Tian S, Chen BW, Ning DM, Guo YM, Zhu WH, Long Y, Xiao W, Deng Z, Lei YC, Tian XF. Frankincense myrrh attenuates hepatocellular carcinoma by regulating tumor blood vessel development through multiple epidermal growth factor receptor-mediated signaling pathways. *World J Gastrointest Oncol* 2022; 14(2): 450-477
**URL:** https://www.wjgnet.com/1948-5204/full/v14/i2/450.htm
**DOI:** https://dx.doi.org/10.4251/wjgo.v14.i2.450

## INTRODUCTION

Primary liver cancer is one of the world's five most prevalent malignant tumors and the second-leading cause of cancer-related deaths. Among liver cancer types, hepatocellular carcinoma (HCC) is the most important histological subtype, and its incidence increases with each passing year. HCC is a highly invasive and metastatic cancer, and patients face a high risk of recurrence and serious complications in the middle and late stages. Worldwide, the prognosis of patients with HCC is extremely poor, with the morbidity and mortality basically the same, seriously threatening human health[1-3].

To support the high proliferation and metastasis rate of HCC, the hypoxia and inflammatory conditions formed during tumor growth cause a magnified response. In addition, the response involves activating oxygen-deficient inducible factors and inflammatory factors and further triggering factors involved in the angiogenesis process, such as VEGF, PDGF and nitric oxide synthase[4]. These responses are conducive to the establishment of an abnormal vascular network, which causes a transition from a nonangiogenic to an angiogenic phenotype. This tumor phenotype is characterized by structural disorder, morphological and functional abnormalities of tumor neovascularization. This transition further exacerbates hypoxic conditions and inflammatory cell penetration, promotes the malignant phenotype and epithelial-mesenchymal transition and contributes to metastatic potential; in addition, the effects of systemic treatments, particularly those dependent on the delivery of macromolecular therapeutic agents to tumors, are impaired, which attenuates the treatment effect[5,6].

Among the pathways triggered by HCC, antiangiogenesis is considered to be a therapeutic target to block tumor growth. In addition, the "tumor blood vessel normalization" concept that has emerged in recent years. VEGF has been at the center of targeted drug development[4,7]. Among the targeted drugs, VEGF/VEGFR inhibitors and tyrosine kinase inhibitors, such as bevacizumab and sorafenib, are widely used in patients with advanced HCC. Recent progress in targeted therapy has directed attention to the treatment of HCC[8,9]. These targeted drugs and therapies have been developed to exert an antiangiogenic effect to promote vascular normalization; however, they induce side effects, such as cardiovascular, cerebrovascular, gastrointestinal tract, hand, foot and skin problems, to different degrees, and they frequently lead to drug resistance[9,10]. Furthermore, these drugs were found to cause the specific enhancement of tumor invasive and metastatic ability, and the low response rate has resulted in the inability of these drugs to prolong the survival of patients with advanced disease. All above leading to uncertainty of their true efficacy and survival benefits, and combined with their high price, has limited their clinical efficacy. Given this situation, there is an urgent need to find new therapeutic agents or components[11-13]. Naturally sourced products or components have curative effects and the advantages of fewer side effects, reduced drug resistance and lower costs[14]. Researchers hope to find therapeutic drugs to target HCC tumor blood vessels.

Frankincense and myrrh are the resins of *Boswellia sylvestris* and *Radix dichotoma*, respectively. They are applied in traditional Chinese medicine (TCM) to treat inflammation and diseases caused by blood stasis. They are the main components of the anti-HCC TCM prescription Xihuang Pill[15-17]. Frankincense, myrrh and their active components show anti-inflammatory and antiproliferative activities in many tumors. For instance, mastic acid, the active component of frankincense, inhibits the growth and metastasis of colorectal cancer by downregulating the expression of biomarkers of inflammation, proliferation, invasion and angiogenesis. Myrrh induces apoptosis and inhibits the proliferation and migration of gastric cancer cells by downregulating cyclooxygenase-2 expression[18,19]. Frankincense and myrrh are always simultaneously used in TCM. The role of frankincense and myrrh in multiple myeloma and liver cancer has been confirmed in previous studies[20,21]. Although frankincense and myrrh have shown promising cancer preventive activity, it has not yet been determined whether frankincense and/or myrrh can inhibit HCC by regulating hypoxia, inflammation and/or tumor blood vessels or their underlying molecular mechanisms.

In our research, we used network pharmacology to predict the potential therapeutic targets of frankincense and myrrh in the treatment of HCC and determined whether frankincense extract, myrrh extract and/or their combination produce anti-HCC effects. We evaluated the effects of these extracts on hypoxia, inflammation and tumor vessels in an HCC model for the first time and proposed a single-step study to establish a potential multimolecular mechanism. This study was performed to clarify the potential therapeutic significance of frankincense and/or myrrh as anti-HCC drug(s) and to promote the development of their natural product components for use in inhibiting tumor blood vessels, which is a promising HCC treatment strategy.

## MATERIALS AND METHODS

### Strategy for screening active components and predicting targets

The active components of frankincense and myrrh were obtained through the Traditional Chinese Medicine Systems Pharmacology Database and Analysis Platform (TCMSP, http://tcmspw.com/tcmsp.php). According to the pharmacokinetic characteristics of these compounds, the active components were characterized for oral bioavailability (OB) ≥ 30% and drug-likeness (DL) ≥ 0.18[22]. Then, the potential targets of the active compounds in frankincense and myrrh in this database were investigated, and the targets were imported into the UniProt database (http://www.UniProt.org) through Perl (https://www.perl.org) to obtain the official gene names of the candidate targets.

### Screening differentially expressed genes in HCC

The GeneCards human gene database (http://www.genecards.org/) and the Comparative Toxicogenomics Database (CTD, http://www.ctdbase.org/) were used to identify differentially expressed genes in HCC. The disease-related genes identified in both GeneCards and CTD were considered HCC-related genes.

### Target cross-validation, construction of an active component-target network and a protein–protein interaction network

Perl was used to intersect the previously obtained differentially expressed genes of HCC with the potential targets of frankincense and myrrh. Thus, the active components and key targets possibly involved in the treatment of HCC with frankincense and myrrh were identified. Cytoscape (version 3.7.0) software was used to construct an active component-target network. The STRING platform (https://string-db.org/) was used to construct and visualize a protein–protein interaction network, wherein the species for network modeling was set to "Homo sapiens" and the minimum interaction score was 0.4[23].

### Functional enrichment analysis of candidate targets

The R packages "BiocManager" and "ClusterProfiler" were used to perform gene ontology (GO) enrichment (to describe the possible cellular environment, molecular function and biological process categories of the gene products) and Kyoto Encyclopedia of Genes and Genomes (KEGG) pathway analysis (to classify the genome annotations and identify the most gene-enriched biological processes) on the basis of the key targets.

### Molecular docking verification

The three-dimensional structures of the active components were obtained from the TCMSP database and considered ligands; the three-dimensional structure of each target protein was obtained from the RCSB Protein Data Bank (PDB, https://www.rcsb.org/), and each was considered a receptor. The AutoDock Tool (version 1.5.6) was used to standardize the receptors and ligands, which were converted into PDBQT format to obtain a three-dimensional grid box for the molecular docking simulation. Molecular docking analysis was performed with AutoDock Vina (Version 1.1.2). PyMOL (https://www.pymol.org/) was used to visualize the docked partners. When the binding energy was less than -5 kcal/mol, the ligand and receptor were considered to be effectively bound[24].

### Chemicals

Frankincense and myrrh extracts (manufacturing certificates: XTY20200827 and TY20200713, with quality inspection carried out with HPLC by the manufacturer) were obtained from New Tianyu Biological Technology (Xianyang, Shanxi, China). Gefitinib (ZD1839) was acquired from TargetMol (Boston, MA, United States). Fetal bovine serum and a mixed penicillin-streptomycin solution were obtained from Thermo Fisher Scientific (Waltham, MA, United States). Phosphate-buffered saline (PBS) and trypsin were obtained from HyClone (Logan, Utah United States). Dimethyl sulfoxide (DMSO) solvent was acquired from Sigma–Aldrich Biotechnology (St. Louis, MO, United States). Glutaraldehyde and paraformaldehyde were purchased from Leagene Biological Technology (Beijing, China). Osmium acid was obtained from Ted Pella (Redding, CA, United States). Enzyme-linked immunosorbent assay (ELISA) kits for TNF-α and HIF-1α were supplied by Cusabio Technology (Wuhan, Hubei, China). Rabbit anti-CD31 polyclonal antibody and goat anti-collagen IV polyclonal antibody were purchased from Abcam (Cambridge, London, United Kingdom), and mouse anti-α-SMA antibody was purchased from Boster Biological Technology (Wuhan, Hubei, China). CoraLite488-conjugated AffiniPure goat anti-mouse IgG (H+L), CoraLite594-conjugated goat anti-rabbit IgG (H+L), fluorescein (FITC)-conjugated AffiniPure donkey anti-goat IgG (H+L) and CoraLite594-conjugated donkey anti-rabbit IgG (H+L) were procured from Proteintech (Danvers, MA, United States). Antibodies against HIF-1α, TNF-α, EGFR, p-EGFR, PI3K, p-PI3K and p-p38 were purchased from Proteintech (Danvers, MA, United States). Antibodies against VEGF, MMP-9, Akt, p-Akt, ERK, p-ERK, p38, JNK, p-JNK, GAPDH and β-actin were purchased from Abcam (Cambridge, London, United Kingdom). Horseradish peroxidase (HRP)-conjugated secondary antibodies were purchased from Proteintech (Danvers, MA, United States). All the other reagents were of analytical grade.

### SMMC-7721 cell culture and treatment

The SMMC-7721 human HCC cell line was commercially acquired and identified from the BeNa Culture Collection Biotechnology Research Institute (Beijing, China, Cell line identification number: 20160628-01). After reseeding, SMMC-7721 cells were cultured in DMEM complete medium (containing 10% fetal bovine serum, 100 U/mL penicillin and 100 μg/mL streptomycin) and placed in a humidified incubator (cultivation environment of 5.0% $CO_2$ and 37°C).

### Preparation of SMMC-7721 cells for subcutaneous transplantation into nude mice and subsequent treatments

Healthy male athymic nude BALB/c (nu/nu) mice (body weight of 18–22 g and aged 4–6 wk) were obtained and raised in miniature cages at the experimental animal science center of Hunan University of Traditional Chinese Medicine. For our research, we followed animal care and used guidelines established by the institution and approved by the Animal Care and Use Committee (approval no. LL2020102801; Changsha, China). All animals were maintained at a room temperature of 25°C, a relative humidity of 45%, and a 12-h light-dark cycle with freely available sterile food and water in an specific-pathogen-free environment. The mice were maintained for 7 consecutive days to adapt to the environment. All parts of the study were conducted under the guidelines for reporting animal studies. The abovementioned SMMC-7721 cells cultured to the exponential growth phase were washed with PBS and resuspended. The concentration of the cells was adjusted to $1 \times 10^7$ cells/mL and prepared in suspension, and 0.1 mL of this cell suspension was injected subcutaneously under the skin of the right armpit area of each nude mouse to establish the models. When the tumor volume was greater than 50 $mm^3$, the mice with these tumors were randomly assigned to 8 groups ($n$ = 5), and they received a low dose of

frankincense extract (LF, equivalent to 1.5 g/kg/d of the native herb), high dose of frankincense extract (HF, equivalent to 3 g/kg/d of the native herbal medicine), low dose of myrrh extract (LM, equivalent to 1.5 g/kg/d of the native herb), high dose of myrrh extract (HM, equivalent to 3 g/kg/d of the native herb), low dose of frankincense + myrrh extracts (LFM, equivalent to 1.5 + 1.5 g/kg/d of each native herb), or high dose of frankincense + myrrh extracts (HFM, equivalent to 3 + 3 g/kg/d of each native herb) with ZD1839 (100 mg/kg/d) in gavage fluid. The mice in the control groups were given saline at a volume equal to the treatment volume. The intervention was maintained for 14 d; the mouse body and tumor weights were regularly measured (every three days), and the tumor volume was calculated (tumor volume = length × width$^2$/2)[25,26]. At the end of the intervention, the mice were euthanized, and the tumor tissues were removed from the mice.

### Histopathological examination

The tumor tissues obtained as described were fixed with 4% paraformaldehyde, and paraffin sections were prepared. After deparaffinization with xylene and dehydration with gradient ethanol, the sections were stained with hematoxylin and eosin, and finally, the slides were dried and mounted. The tissue structure of each sample was microscopically inspected, and images were collected.

### ELISAs

The tumor tissues were cut into pieces, homogenized and centrifuged, and the tissue supernatant was collected. According to the protocols of the ELISA kit manufacturer, the levels of HIF-1α and TNF-α were quantified.

### Immunofluorescence staining

The treated tumor tissue sections were subjected to thermal antigen retrieval with EDTA buffer (pH = 9.0) and washed 3 times with 0.01 M PBS (pH = 7.4). Then, the cells were treated with 0.1% NaBH4 (30 min incubation) and Sudan black dye solution (5 min incubation) to reduce autofluorescence, and 5% BSA was selected to avoid nonspecific staining (it was allowed to bind the sections for 1 h at 37°C). To evaluate the microvascular condition of the tumor tissue, the sections were combined with the corresponding primary antibodies: rabbit anti-CD31 (1:50, endothelial marker), mouse anti-α-SMA (1:50, pericyte marker) and goat anti-collagen IV (1:50, basement membrane marker) and incubated overnight at 4°C for labeling. After washing with PBS, CoraLite488-conjugated AffiniPure goat anti-mouse IgG (H+L) (1:500), CoraLite594-conjugated goat anti-rabbit IgG (H+L) (1:500) and FITC-conjugated AffiniPure donkey anti-goat IgG (H+L) (1:100) were added as secondary antibodies and incubated at 37°C for 90 min. An upright fluorescence microscope and imaging system (Motic, Fujian, China) was used for visualization, image acquisition and analysis of fluorescence signals. By analyzing the levels of different fluorescence intensities, the endothelial cell (EC) area (red), pericyte area (green) and basement membrane area (green) were evaluated. The pericyte coverage of tumor microvessels was evaluated by integrating two-dimensional images, quantifying the fluorescence in each area, reported as the pericyte area (green area)/EC area (red area).

### Transmission electron microscopy

Samples fixed with glutaraldehyde were rinsed with phosphoric acid buffer, fixed with osmic acid, dehydrated with an ethanol gradient, infiltrated and embedded with resin that was then polymerized. The ultramicrotome-cut sections were prepared and double stained with 3% lead citrate. Finally, the samples were observed and visualized by transmission electron microscopy (Hitachi, Chiyoda-ku, Tokyo, Japan).

### Reverse transcription-quantitative polymerase chain reaction assay

The extraction and purification of total RNA from tumor tissue was carried out with TRIzol reagent (Invitrogen, Waltham, MA, United States). cDNA was obtained by the reverse transcription of the total RNA using an RNA reverse transcription kit (CWBio tech, Beijing, China). Quantitative polymerase chain reaction (qPCR) was carried out using the SYBR Green chemistry method on a QuantStudio 6 Flex Real-Time PCR system (Thermo Fisher Scientific, Waltham, MA, United States), in which the amplification procedure was executed at 95°C for 10 min, followed by 40 cycles at 95°C for 15 s and 60°C for 60 s. GAPDH was selected as the internal reference, and the primers were designed by Premier 5.0 software (Table 1).

**Table 1 The RNA sequences used in this study**

| Name | Primer sequence | Primer length |
|---|---|---|
| HIF-1α | F→TCCAGCAGACCCAGTTACAGA; R→GCCACTGTATGCTGATGCCTT | 182bp |
| TNF-α | F→AGCACAGAAAGCATGATCCG; R→CACCCCGAAGTTCAGTAGACA | 162bp |
| VEGF | F→GAACCAGACCTCTCACCGGAA; R→ACCCAAAGTGCTCCTCGAAG | 135bp |
| MMP-9 | F→GCCCTGGAACTCACACGACA; R→GTAGCCCACGTCGTCCACC | 139bp |
| GAPDH | F→GCGACTTCAACAGCAACTCCC; R→CACCCTGTTGCTGTAGCCGTA | 122bp |

### *Western blot analysis*

On ice, the cryopreserved tumor tissue was homogenized by grinding, and the total protein was extracted with radioimmunoprecipitation assay lysis buffer (Applygen Technologies Inc., Beijing, China). A bicinchoninic acid protein detection kit (Thermo Fisher Scientific, Waltham, MA, United States) was used to determine the protein concentration according to the manufacturer's protocol. Equal amounts of protein samples were separated by sodium dodecyl sulfate–polyacrylamide gel electrophoresis, transferred to a polyvinylidene fluoride membrane and blocked with 5% BSA in PBS for 1 h. The membrane was incubated overnight at 4°C with the following specific primary antibodies against HIF-1α (1:1000), TNF-α (1:1000), VEGF (1:1000), MMP-9 (1:2000), EGFR (1:1000), p-EGFR (1:1000), PI3K (1:5000), p-PI3K (1:800), Akt (1:1000), p-Akt (1:5000), p38 (1:5000), p-p38 (1:1000), ERK (1:2000), p-ERK (1:3000), JNK (1:10000), p- JNK (1:2000), β-actin (1:5000) and GAPDH (1:5000). Furthermore, the membranes were incubated with the corresponding HRP-conjugated secondary antibody, anti-rabbit IgG (1:6000) or anti-mouse IgG (1:5000) antibody, for 2 h. A SuperSignal enhanced chemiluminescence detection kit (Thermo Fisher Scientific, Waltham, MA, United States) with a Bio–Rad ChemiDoc XRS+ System (Bio–Rad Laboratories, Inc., Hercules, CA, United States) was used to develop the immunoreactivity for blot detection and visualization. β-Actin and GAPDH were used as the protein loading controls.

### *Statistical analyses*

The mean ± SE were applied to present quantitative data. One-way analysis of variance and Tukey's post-test were used to confirm their significant differences, where a $P$ value less than 0.05 ($P < 0.05$) was considered to be significantly different. The statistical analysis software GraphPad Prime 8.3.1 (GraphPad Software Inc., La Jolla, CA, United States) was used for all statistical tests.

## RESULTS

### *Network pharmacology-based analysis*

**Identification of frankincense and myrrh targets in HCC:** The active components of frankincense and myrrh were obtained from the TCMSP database. After eliminating overlapping compounds, a total of 58 candidate bioactive components were identified, and 367 targets were retrieved. After merging duplicate lists, 177 targets were identified (Table 2). Furthermore, as shown in Figure 1A, 6900 human genes related to HCC were collected from the GeneCards and CTD databases, and after identifying overlapping genes and merging the data, the genes were mapped to the 177 candidate targets corresponding to frankincense and myrrh. It was concluded that the treatment of HCC by frankincense and myrrh is associated with 151 targets of 35 active components.

### *Construction of an active component-target network and a protein–protein interaction network*

An active component target network diagram of frankincense and myrrh in the treatment of HCC was constructed for characterization (Figure 1B). The main active components highly effective against HCC in myrrh were quercetin (MOL000098, degree = 126), beta-sitosterol (MOL000358, degree = 19), stigmasterol (MOL000449, degree = 19), ellagic acid (MOL001002, degree = 18) and pelargonidin (MOL001004, degree = 14); in frankincense, the highly effective anti-HCC compounds were

**Table 2 The effective candidate ingredients of frankincense and myrrh**

| Mol ID | Molecule name | OB (%) | DL | Medicine |
|---|---|---|---|---|
| MOL001215 | Tirucallol | 42.12 | 0.75 | Frankincense |
| MOL001241 | O-acetyl-α-boswellic acid | 42.73 | 0.70 | Frankincense |
| MOL001243 | 3alpha-Hydroxy-olean-12-en-24-oic-acid | 39.32 | 0.75 | Frankincense |
| MOL001255 | Boswellic acid | 39.55 | 0.75 | Frankincense |
| MOL001263 | 3-oxo-tirucallic, acid | 42.86 | 0.81 | Frankincense |
| MOL001265 | Acetyl-alpha-boswellic,acid | 42.73 | 0.70 | Frankincense |
| MOL001272 | Incensole | 45.59 | 0.22 | Frankincense |
| MOL001295 | Phyllocladene | 33.40 | 0.27 | Frankincense |
| MOL000098 | Quercetin | 46.43 | 0.28 | Myrrh |
| MOL000358 | Beta-sitosterol | 36.91 | 0.75 | Myrrh |
| MOL000449 | Stigmasterol | 43.83 | 0.76 | Myrrh |
| MOL000490 | Petunidin | 30.05 | 0.31 | Myrrh |
| MOL000979 | 2-methoxyfuranoguaia-9-ene-8-one | 66.18 | 0.18 | Myrrh |
| MOL000988 | 4,17(20)-(cis)-pregnadiene-3,16-dione | 51.42 | 0.48 | Myrrh |
| MOL000996 | Guggulsterol IV | 33.59 | 0.74 | Myrrh |
| MOL001001 | Quercetin-3-O-β-D-glucuronide | 30.66 | 0.74 | Myrrh |
| MOL001002 | Ellagic acid | 43.06 | 0.43 | Myrrh |
| MOL001004 | Pelargonidin | 37.99 | 0.21 | Myrrh |
| MOL001006 | Poriferasta-7,22E-dien-3beta-ol | 42.98 | 0.76 | Myrrh |
| MOL001009 | Guggulsterol-VI | 54.72 | 0.43 | Myrrh |
| MOL001013 | Mansumbinoic acid | 48.10 | 0.32 | Myrrh |
| MOL001019 | (7S,8R,9S,10R,13S,14S,17Z)-17-ethylidene-7-hydroxy-10,13-dimethyl-1,2,6,7,8,9,11,12,14,15-decahydrocyclopenta(a)phenanthrene-3,16-dione | 35.75 | 0.48 | Myrrh |
| MOL001021 | 7β,15β- dihydroxypregn-4-ene-3,16-dione | 43.11 | 0.51 | Myrrh |
| MOL001022 | 11α-hydroxypregna-4,17(20)-trans-diene-3,16-dione | 36.62 | 0.47 | Myrrh |
| MOL001026 | Myrrhrrhanol C | 39.96 | 0.58 | Myrrh |
| MOL001027 | Myrrhrrhanone A | 40.25 | 0.63 | Myrrh |
| MOL001028 | (8R)-3-oxo-8-hydroxy-polypoda-13E,17E,21-triene | 44.83 | 0.59 | Myrrh |
| MOL001029 | Myrrhrrhanones B | 34.39 | 0.67 | Myrrh |
| MOL001031 | Epimansumbinol | 61.81 | 0.40 | Myrrh |
| MOL001033 | Diayangambin | 63.84 | 0.81 | Myrrh |
| MOL001040 | (2R)-5,7-dihydroxy-2-(4-hydroxyphenyl)chroman-4-one | 42.36 | 0.21 | Myrrh |
| MOL001045 | (13E,17E,21E)-8-hydroxypolypodo-13,17,21-trien-3-one | 44.34 | 0.58 | Myrrh |
| MOL001046 | (13E,17E,21E)-polypodo-13,17,21-triene-3,18-diol | 39.96 | 0.58 | Myrrh |
| MOL001049 | 16-hydroperoxymansumbin-13(17)-en-3β-ol | 41.05 | 0.49 | Myrrh |
| MOL001052 | Mansumbin-13(17)-en-3,16-dione | 41.78 | 0.45 | Myrrh |
| MOL001061 | (16S,20R)-dihydroxydammar-24-en-3-one | 37.34 | 0.78 | Myrrh |
| MOL001062 | 15α-hydroxymansumbinone | 37.51 | 0.44 | Myrrh |
| MOL001063 | 28-acetoxy-15α-hydroxymansumbinone | 41.85 | 0.67 | Myrrh |
| MOL001069 | 3β-acetoxy-16β,20(R)-dihydroxydammar-24-ene | 38.72 | 0.81 | Myrrh |

| | | | | |
|---|---|---|---|---|
| MOL001088 | 1α-acetoxy-9,19-cyclolanost-24-en-3β-ol | 44.40 | 0.78 | Myrrh |
| MOL001092 | {(3R,5R,8R,9R,10R,13R,14R,17S)-17-[(2S,5S)-5-(2-hydroxypropan-2-yl)-2-methyloxolan-2-yl]-4,4,8,10,14-pentamethyl-2,3,5,6,7,9,11,12,13,15,16,17-dodecahydro-1H-cyclopenta(a)phenanthren-3-yl} acetate | 33.07 | 0.80 | Myrrh |
| MOL001093 | Cabraleone | 36.21 | 0.82 | Myrrh |
| MOL001095 | Isofouquierone | 40.95 | 0.78 | Myrrh |
| MOL001126 | [(5aS,8aR,9R)-8-oxo-9-(3,4,5-trimethoxyphenyl)-5,5a,6,9-tetrahydroisobenzofurano(6,5-f)(1,3)benzodioxol-8a-yl] acetate | 44.08 | 0.90 | Myrrh |
| MOL001131 | Phellamurin_qt | 56.60 | 0.39 | Myrrh |
| MOL001138 | (3R,20S)-3,20-dihydroxydammar-24-ene | 37.49 | 0.75 | Myrrh |
| MOL001145 | (20S)-3β-acetoxy-12β,16β,25-tetrahydroxydammar-23-ene | 34.89 | 0.82 | Myrrh |
| MOL001146 | (20S)-3β,12β,16β,25-pentahydroxydammar-23-ene | 37.94 | 0.75 | Myrrh |
| MOL001147 | (20R)-3β-acetoxy-16β-dihydroxydammar-24-ene | 40.36 | 0.82 | Myrrh |
| MOL001148 | 3β-hydroxydammar-24-ene | 40.27 | 0.82 | Myrrh |
| MOL001156 | 3-methoxyfuranoguaia-9-en-8-one | 35.15 | 0.18 | Myrrh |
| MOL001164 | [(5S,6R,8R,9Z)-8-methoxy-3,6,10-trimethyl-4-oxo-6,7,8,11-tetrahydro-5H-cyclodeca(b)furan-5-yl] acetate | 34.76 | 0.25 | Myrrh |
| MOL001175 | Guggulsterone | 42.45 | 0.44 | Myrrh |

boswellic acid (MOL001255, degree = 3), 3-alpha-hydroxy-olean-12-en-24-oic-acid (MOL001243, degree = 3) and platylene (MOL001241, degree = 2). The constructed protein–protein interaction network (Figure 1C-D) revealed that AKT1 (degree = 104), IL-6 (degree = 97), VEGF (degree = 89), EGFR (degree = 76) and MAPK1 (degree = 76) were the high-degree targets, indicating that these highly correlated targets in the network may play a basic therapeutic role in treatment by frankincense and/or myrrh in HCC.

### *Enrichment analysis of the key frankincense and myrrh targets in HCC*

To reveal the biological characteristics of anti-HCC targets of frankincense and myrrh, GO and KEGG enrichment analyses were performed. A total of 2053 GO terms were obtained. Among them, the target genes in the MF category (molecular function, 160) were mainly enriched in DNA-binding transcription factor binding, ligand-activated transcription factor activity, cytokine receptor binding, phosphatase binding and antioxidant activity; in the BP category (biological process, 1850), the target genes were mainly enriched in the response to oxygen level, hypoxia, oxygen content reduction, lipopolysaccharide and chemical stress; and in the CC category (cellular components, 43), the target genes were mainly enriched in transcriptional regulatory complex, serine/threonine protein kinase complex, protein kinase complex, *etc.* (Figure 2A-C). To explore the potential pathway of frankincense and myrrh compounds in HCC, KEGG pathway analysis was carried out (Figure 2D). The results showed that target genes were significantly enriched in the MAPK signaling pathway, HIF-1 signaling pathway, platinum resistance, EGFR tyrosine kinase inhibitor resistance, ErbB signaling pathway, *etc.*

### *Molecular docking analysis*

According to network analysis, molecular docking was used to verify the binding of the key components of frankincense (boswellic acid, 3alpha-hydroxy-olean-12-en-24-oic-acid and platylene) and myrrh (quercetin, beta-sitosterol and stigmasterol) with key targets (AKT1, VEGFA and EGFR). The binding energy was calculated to assess the degree to which a component bound with a protein target. A lower binding energy indicates higher stability. The results showed that the representative components of frankincense and myrrh bind with high affinity to the active sites of protein targets. Boswellic acid (Figure 3A-C) and stigmasterol (Figure 3D-F) both showed strong affinity for their respective targets. The compounds showed the greatest affinity for EGFR (Table 3).

### *Experimental Validation*

**Frankincense and/or myrrh inhibits tumor growth in nude mouse models with subcutaneously transplanted human HCC tumor cells *in vivo*:** To further verify and evaluate the effect of frankincense and/or myrrh in HCC treatment, human

**Table 3 Virtual docking of biologically active ingredients from frankincense and myrrh for hepatocellular carcinoma targets**

| Mol ID | Molecule name | Scores/(kcal·mol$^{-1}$) | | |
|---|---|---|---|---|
| | | AKT1 | VEGFA | EGFR |
| MOL000098 | Quercetin | -7.6 | -5.7 | -7.2 |
| MOL000358 | Beta-sitosterol | -8.1 | -6.9 | -9.2 |
| MOL000449 | Stigmasterol | -8.6 | -6.8 | -9.6 |
| MOL001243 | 3alpha-Hydroxy-olean-12-en-24-oic-acid | -8.7 | -7.1 | -8.3 |
| MOL001255 | Boswellic acid | -8.8 | -7.0 | -9.3 |

subcutaneously transplanted HCC tumor models were constructed. The tumors in the model control group continued to grow large. In contrast, in the intervention groups, the tumors did not increase significantly during the treatment time (Figure D). By the end of the treatment course, compared with that in the model control group, the tumor size of each drug intervention group was significantly reduced ($P < 0.05$; Figure 4A and C). The tumor inhibition rate was further studied to evaluate the effect of the extracts on tumor growth {tumor inhibition rate (%) = [(average tumor volume of the model control group-average tumor volume of the treatment group)/average tumor volume of the model control group] × 100%}. The tumor inhibition rates of LF, HF, LM, HM, LFM, HFM and ZD1839 were 29.8%, 33.2%, 29.9%, 44.8%, 36.9%, 45.6% and 49.1%, respectively. These observations indicated that frankincense and/or myrrh treatments significantly inhibited the size and growth rate of tumors in HCC models. In addition, the body weights of the mice in the model control and treatment groups were similar (Figure 4B), indicating that there was no serious toxicity induced during the frankincense and/or myrrh intervention.

A histological examination showed that most of the tumor cells in the model control group were large with abnormal morphology, large nuclei and obvious nucleoli. Mitotic features were more common, and evidence of mitosis and necrosis was observed under the microscope, indicating that the features of the tumor in this study were similar to general tumor characteristics. In contrast, the morphology of the tumor cells in the treatment groups was relatively regular, with few mitotic images or necrotic areas (Figure 4E). These results proved that frankincense and/or myrrh has a significant inhibitory effect on the growth of HCC *in vivo*.

### *Frankincense and/or myrrh improves tumor vascular morphology*

CD31 specifically labels endothelial blood vessels, including mature and immature blood vessels, which is measured to distinguish blood vessels from peripheral cancer cells. In addition, α-SMA is a specific biomarker of perivascular cells covering mature blood vessels[27]. The assay results in this study showed that CD31 (red) was overexpressed in the tumors in the model control group, and the vascular morphology showed marked hypertrophy, malformation and discontinuous lumen. The expression of CD31 in each intervention group was decreased to varying degrees ($P < 0.05$). The intervention group treated with either frankincense plus myrrh or the inhibitor intervention group exhibited the thinning of the tube wall and a continuous lumen, which proves that frankincense plus myrrh in combination and the inhibitor may reduce tumor angiogenesis (Figure 5A and B).

Pericytes (green α-SMA) can be seen around the blood vessel (red, CD31). In the model control group, the thickness of the pericytes was uneven; the lumen was discontinuous, and the pericytes did not completely surround the vascular ECs. In each drug intervention group, the area with pericytes was increased, the area thickness was increased, the connection between areas was more complete, and the coverage of the pericytes was increased significantly ($P < 0.05$). Among the treatment groups, the pericyte coverage in the HFM group was significantly higher than that of the single-drug intervention groups ($P < 0.05$), and complete and continuous vascular endothelial cells were continuously covered by a layer of uniform pericytes, which were closely connected to each other, showing regularity and a closed luminal shape. The results showed that frankincense and/or myrrh might effectively increase the coverage of tumor perivascular cells and promote blood vessel maturation (Figure 5A and C).

The basement membrane is an important factor in blood vessel maturity and functional integrity[28]. Collagen IV labeled with green fluorescence enabled an examination of the morphology and expression of the basement membrane (Figure 6).

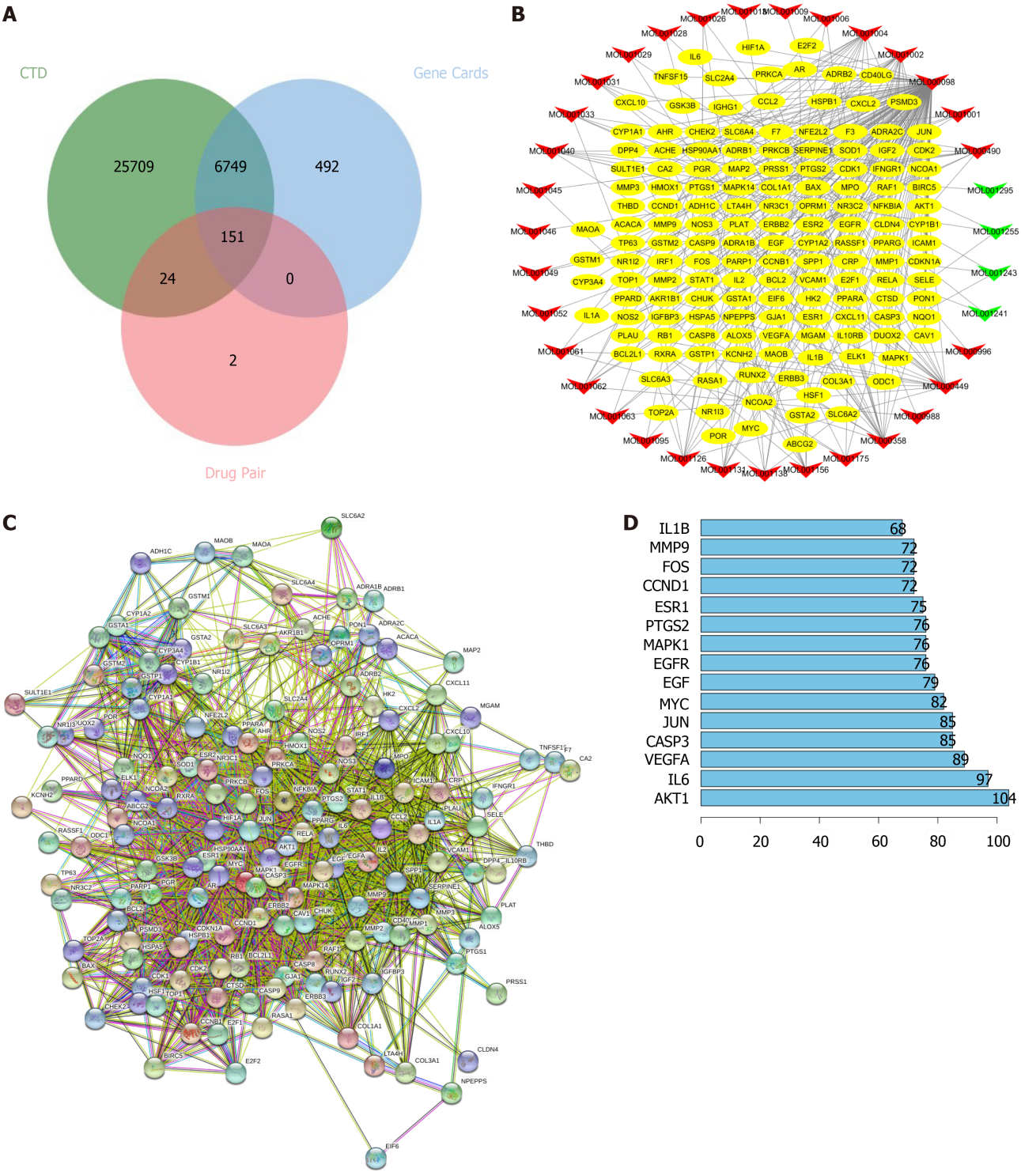


**Figure 1 Active component target network and protein-protein interaction network of frankincense and myrrh in the treatment of hepatocellular carcinoma.** A: Wayne diagram of the targets; B: Compound-target network. Yellow oval node represents the key target, the green node represents the active ingredient of frankincense, and the red node represents the active ingredient of myrrh, The edges represent the interactions between them; C: Protein-protein interaction network. Circular nodes represent targets and edges represent interactions; D: The bar chart of the sorting of the core target. The abscissa represents the number of nodes, and the ordinate is the name of the core target.

In the model control group, the expression of collagen IV was high; the basement membrane distribution was scattered, and its thickness was uneven; in contrast, the expression of collagen IV in each drug intervention group was decreased to varying degrees ($P < 0.01$), and the basement membrane distribution was thinner. The expression of collagen IV in the ZD1839 group tended to be downregulated ($P < 0.001$), indicating that targeting EGFR had a certain effect on the vascular basement membrane, but the HFM group showed a more uniform and regular basement membrane distribution and a closed and regular lumen morphology. These findings

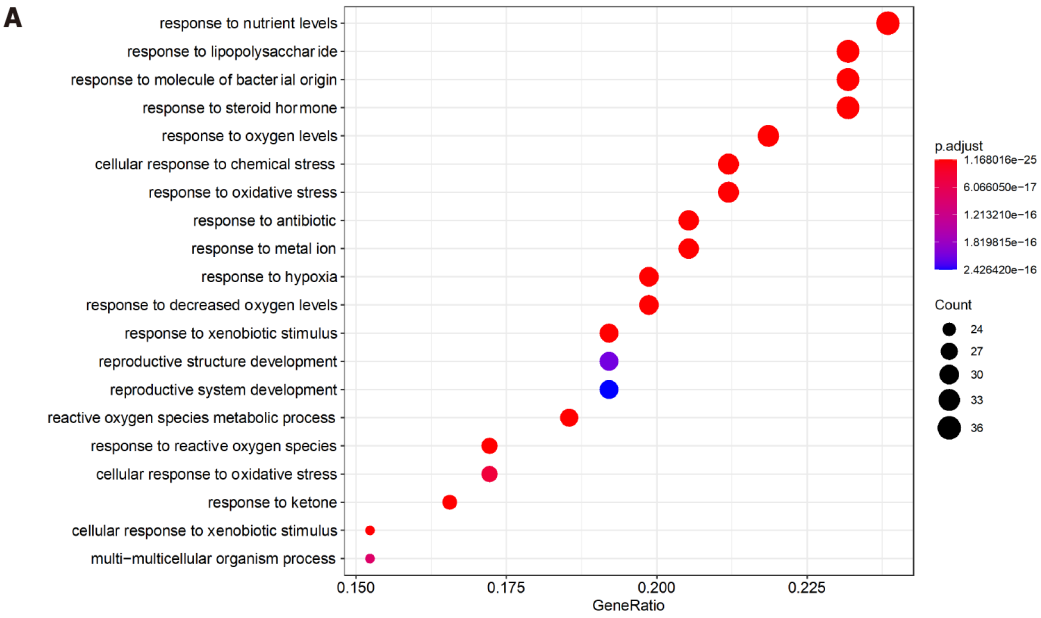
A
response to nutrient levels
response to lipopolysaccharide
response to molecule of bacterial origin
response to steroid hormone
response to oxygen levels
cellular response to chemical stress
response to oxidative stress
response to antibiotic
response to metal ion
response to hypoxia
response to decreased oxygen levels
response to xenobiotic stimulus
reproductive structure development
reproductive system development
reactive oxygen species metabolic process
response to reactive oxygen species
cellular response to oxidative stress
response to ketone
cellular response to xenobiotic stimulus
multi-multicellular organism process
0.150
0.175
0.200
0.225
GeneRatio
p.adjust
1.168016e-25
6.066050e-17
1.213210e-16
1.819815e-16
2.426420e-16
Count
24
27
30
33
36

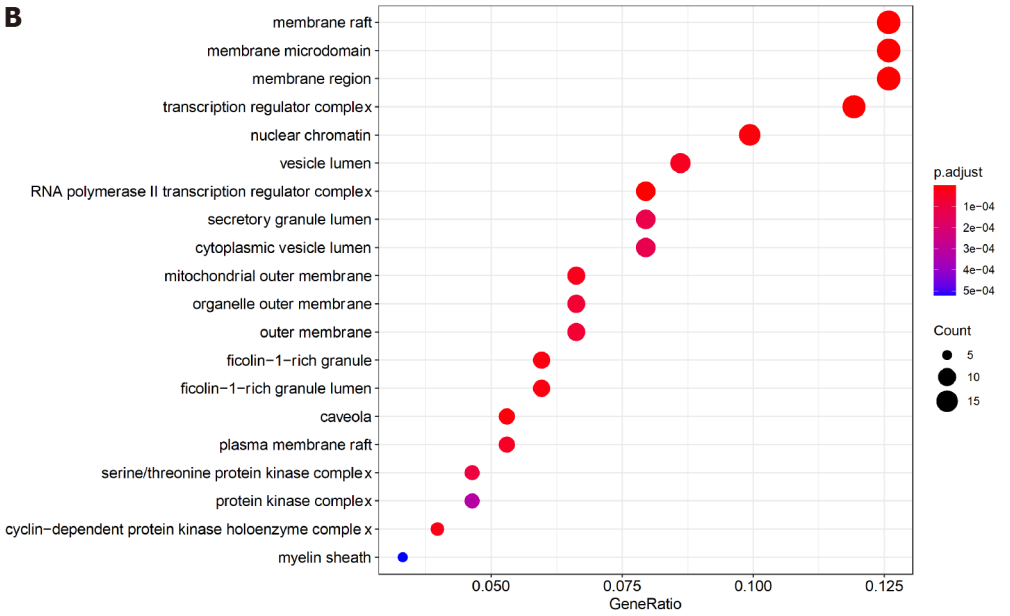
B
membrane raft
membrane microdomain
membrane region
transcription regulator complex
nuclear chromatin
vesicle lumen
RNA polymerase II transcription regulator complex
secretory granule lumen
cytoplasmic vesicle lumen
mitochondrial outer membrane
organelle outer membrane
outer membrane
ficolin-1-rich granule
ficolin-1-rich granule lumen
caveola
plasma membrane raft
serine/threonine protein kinase complex
protein kinase complex
cyclin-dependent protein kinase holoenzyme complex
myelin sheath
0.050
0.075
0.100
0.125
GeneRatio
p.adjust
1e-04
2e-04
3e-04
4e-04
5e-04
Count
5
10
15

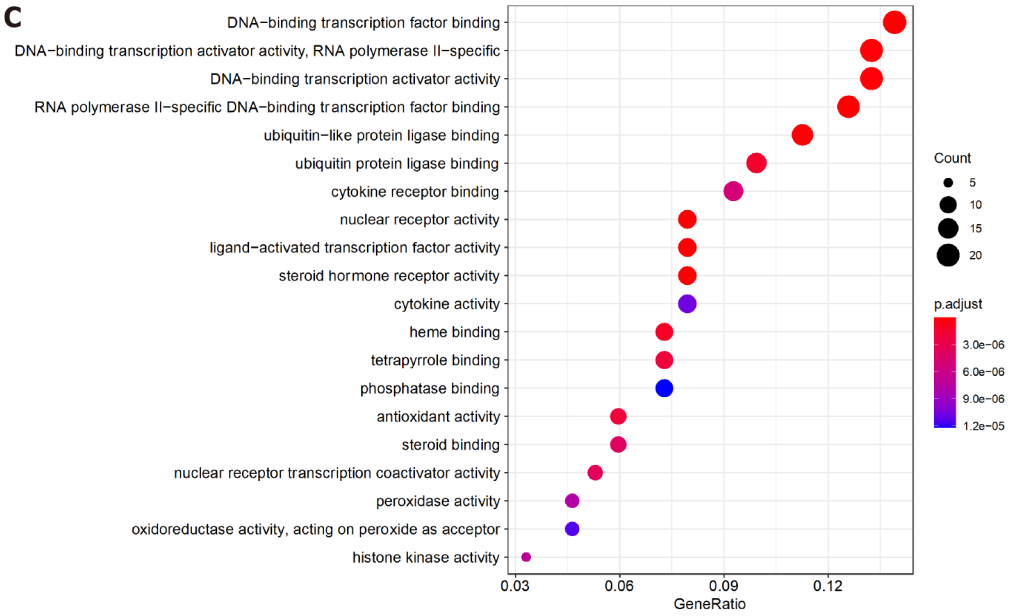
C
DNA-binding transcription factor binding
DNA-binding transcription activator activity, RNA polymerase II-specific
DNA-binding transcription activator activity
RNA polymerase II-specific DNA-binding transcription factor binding
ubiquitin-like protein ligase binding
ubiquitin protein ligase binding
cytokine receptor binding
nuclear receptor activity
ligand-activated transcription factor activity
steroid hormone receptor activity
cytokine activity
heme binding
tetrapyrrole binding
phosphatase binding
antioxidant activity
steroid binding
nuclear receptor transcription coactivator activity
peroxidase activity
oxidoreductase activity, acting on peroxide as acceptor
histone kinase activity
0.03
0.06
0.09
0.12
GeneRatio
Count
5
10
15
20
p.adjust
3.0e-06
6.0e-06
9.0e-06
1.2e-05

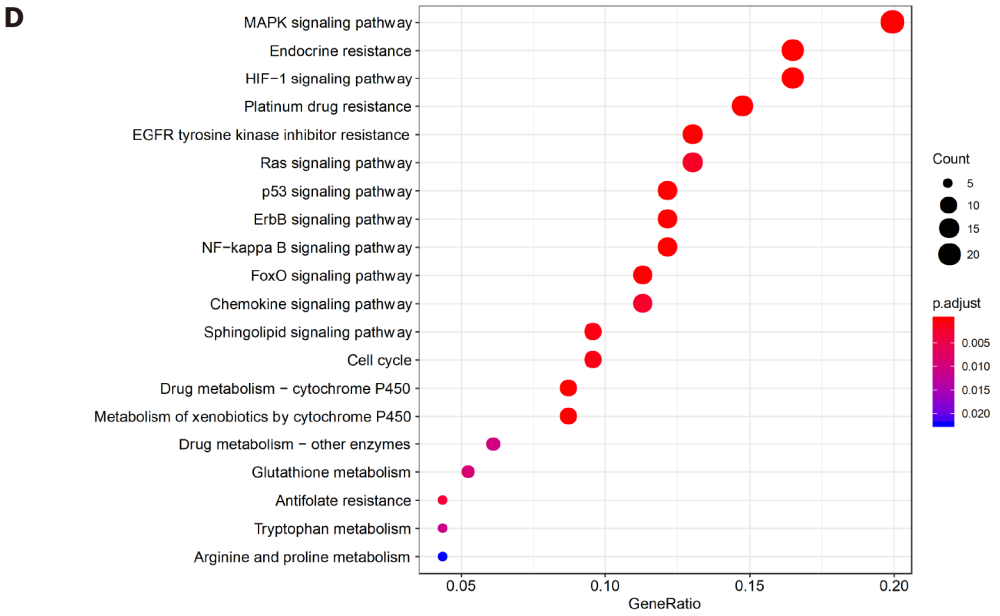


**Figure 2 Enrichment analysis of frankincense and myrrh key targets on hepatocellular carcinoma.** A-C: GO analysis; A: Biological process; B: Cellular component; C: Molecular function; D: KEGG analysis.

indicate that frankincense and/or myrrh may affect the distribution and morphology of the basement membrane of tumor vessels.

The ultrastructure of tumor vascular cells was observed by TEM (Figure 7). In the model control group (Figure 7A), the connections between tumor vascular cells were loose, the cell gap was significantly enlarged, and the cell morphology was changed. Compared with that of the control, the effect of frankincense and myrrh treatment on EC junctions and pericytes (Figure 7B) caused significantly enhanced integrity of the surrounding and basement membranes, and the cell-to-cell connection was tight, indicating that frankincense and myrrh enhanced the morphological structure of tumor blood vessel cells.

### *Frankincense and/or myrrh inhibits the secretion of HIF-1α and TNF-α*

HIF-1α is a recognized core mediator in the hypoxic environment of tumors. The proinflammatory cytokine TNF-α is the main mediator of tumor acceleration. These factors function together to form a signal transduction circuit and activate VEGF, and they are closely related to HCC angiogenesis[29,30]. To determine whether frankincense and/or myrrh has an effect on local hypoxia and inflammation-related factors in tumors, the main markers of these conditions, namely, hypoxia-inducible factor HIF-1α and proinflammatory cytokine TNF-α, were extensively studied. The results are shown in Figure 8A and B. ELISAs revealed that, compared with the model control group, the content of HIF-1α and TNF-α in the tumor body in each intervention group was significantly reduced ($P < 0.05$); compared with ZD1839 group, in both frankincense plus myrrh groups (LFM and HFM) groups, the degree of intervention on each factor was the same, indicating that frankincense and/or myrrh effectively enhanced the secretion of hypoxia-inducible factor HIF-1α and inflammatory factors TNF-α in the subcutaneously transplanted HCC tumors in nude mice.

These results were confirmed by the WB and RT-qPCR results. As shown in Figure 8C-G, compared with those in the model control group, the protein and mRNA expression levels of HIF-1α and TNF-α in the tumor body in each intervention group were significantly downregulated ($P < 0.05$); similarly, in both frankincense plus myrrh intervention groups (LFM and HFM) and in the ZD1839 group, no significant difference was found in the degree of intervention on HIF-1α or TNF-α expression. These results showed that frankincense and/or myrrh effectively downregulated the protein and mRNA expression levels of HIF-1α and TNF-α in HCC subcutaneously transplanted tumors in nude mice.

### *Frankincense plus myrrh inhibits the expression of VEGF and MMP-9*

VEGF is the principal stimulator of tumor angiogenesis, and MMP-9 can cause abnormal proliferation of tumor blood vessels[31]. Therefore, with the prediction targets identified through network pharmacology, we sought to clarify the influence of

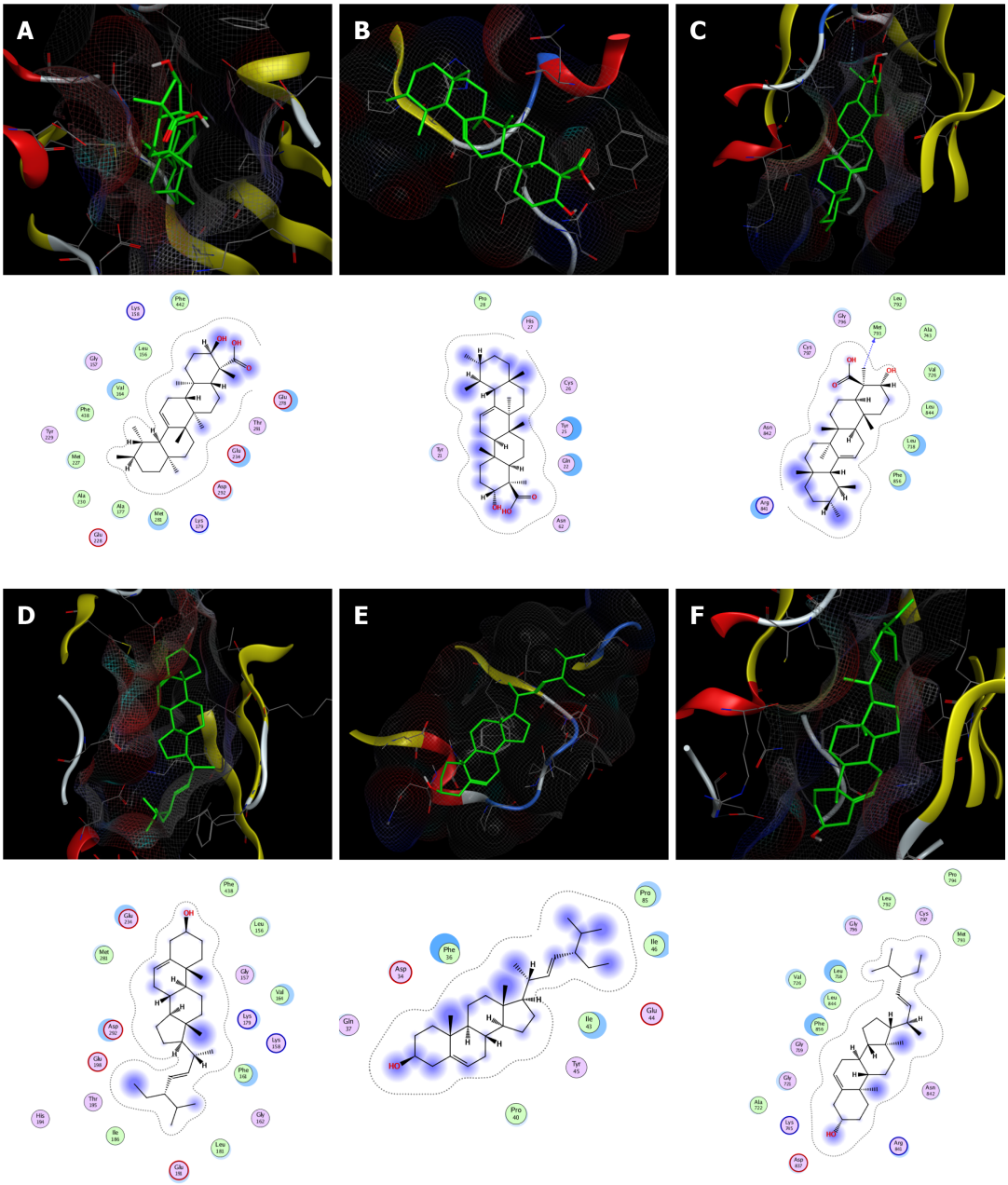


**Figure 3 The docking model of boswellic acid and stigmasterol with key targets.** A: Boswellic acid with AKT1; B: Boswellic acid with VEGFA; C: Boswellic acid with EGFR; D: Stigmasterol with AKT1; E: Stigmasterol with VEGFA; F: Stigmasterol with EGFR.

frankincense and/or myrrh on tumor vascular-related factors, namely, the main markers VEGF and MMP-9.

As shown in Figure 9, compared with those in the model control group, in each intervention group, the protein and mRNA expression levels of VEGF and MMP-9 in the tumor were significantly downregulated ($P < 0.05$), and they were the lowest in the ZD1839 group. There was no significant difference in VEGF and MMP-9 intervention between the ZD1839 group and the frankincense plus myrrh intervention groups (LFM and HFM); compared with the effect of frankincense or myrrh treatment alone, the combined frankincense and myrrh treatment had a greater effect with regard to reducing the expression of VEGF and MMP-9 ($P < 0.05$). These results show that the inhibition of EGFR can interfere with the expression of VEGF and MMP-9, and frankincense plus myrrh can effectively reduce the protein and mRNA expression of VEGF and MMP-9 in HCC subcutaneously transplanted tumors.

### *Frankincense and/or myrrh has a regulatory effect on multiple signaling pathways*

Changes in the vascular morphology of HCC are thought to be related to a variety of signaling pathways in the angiogenic process. Among these pathways, the EGFR,

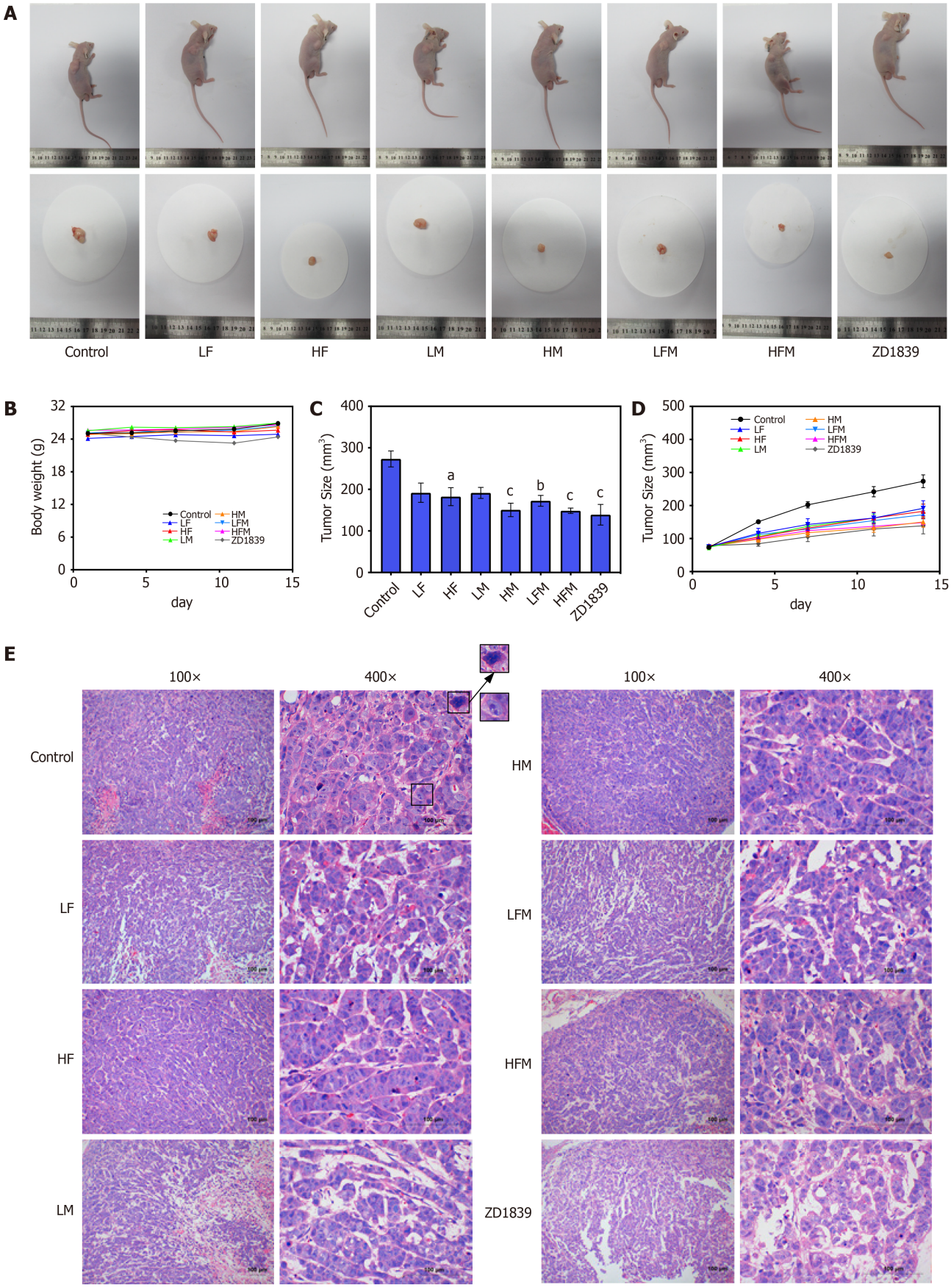


**Figure 4 The effect of frankincense and/or myrrh in the tumor growth of human hepatocellular carcinoma subcutaneously transplanted tumor models.** A: Representative images of tumor size at the end of the experiment; B: Animal weight during the entire oral treatment process; C: Statistical graph of tumor size at the end of the experiment; D: Changes in tumor size during the entire oral treatment process; E: H-E staining of tumors in each group (100×, 400×), scale bars: 100 μm. LF: Low dose of frankincense extract; HF: High dose of frankincense extract; LM: Low dose of myrrh extract; HM: High dose of myrrh extract;

LFM: Low dose of frankincense + myrrh extracts; HFM: High dose of frankincense + myrrh extracts. Data represents the mean ± SE. Compared with the model control, $^{a}P < 0.05$, $^{b}P < 0.01$, $^{c}P < 0.001$.

PI3K/Akt and MAPK signaling cascades are closely related to tumor blood vessels[32-34]. In our network pharmacology predictions, these signaling pathways and related proteins were the key pathways and protein targets of frankincense and/or myrrh anti-HCC effects. To further clarify and verify the signaling pathways potentially affected by frankincense and/or myrrh intervention, we studied whether these compounds have a regulatory effect on the abovementioned signaling pathways.

As depicted in Figure 10, upon extract intervention, compared with the model control group, the phosphorylation levels of EGFR, PI3K, Akt, ERK, p38 and JNK in the experimental groups were significantly downregulated ($P < 0.05$). Among these proteins, the levels of these phosphorylated proteins were lowest in the ZD1839 group, and the expression level of both frankincense plus myrrh interventions (LFM and HFM) was not significantly different from that of ZD1839. Frankincense or myrrh used alone had a less profound downregulating effect on the level of protein phosphorylation than their combined use and showed a significantly different effect on PI3K/Akt and MAPK pathway-related proteins ($P < 0.05$). These observations prove that the inhibition of EGFR downregulates the phosphorylation-induced activation of PI3K/Akt and MAPK and that frankincense plus myrrh effectively regulates the activation of EGFR and the PI3K/Akt and MAPK signaling pathways in subcutaneously transplanted HCC tumors in nude mice.

## DISCUSSION

HCC is an urgent global public health problem with a complex developmental process that is often associated with multiple pathways and proteins. Despite improvements in the understanding of the pathophysiological mechanisms of HCC, no practical breakthroughs have been achieved in HCC treatment[1,4]. TCM, as a complementary and alternative therapy for treating HCC, shows a multicomponent, multitarget and multipathway therapeutic pattern in its mechanism of action. In this study, the focus of investigation was the effects and mechanisms of frankincense plus myrrh in Xihuang Pill on HCC through network pharmacological prediction, molecular docking and *in vivo* model validation (Figure 11).

Within the active component-target network, highly active components may play the main therapeutic role upon frankincense plus myrrh treatment in HCC, with boswellic acid (MOL001255, OB = 39.55%, DL = 0.75) being the main active component in frankincense. Previous studies have indicated that boswellic acid exerts a negative effect on tumor growth, metastasis and microangiogenesis. Boswellic acid reduces the levels of phosphorylated ERK and p38, inhibiting the expression of TNF-α, CD31, MMP-9 and VEGF[18,35]. The main active component in myrrh, stigmasterol (MOL000449, OB = 43.83%, DL = 0.76), is known to inhibit tumor growth by similarly significantly reducing TNF-α transcription levels and Akt phosphorylation levels, reducing CD31-positive vascular content and macrophage recruitment for targeting tumor ECs and exerting an anti-inflammatory effect[36]. Studies have also demonstrated that stigmasterol in combination with cisplatin can inhibit cisplatin chemoresistance[37].

From the results of the drug target prediction, pathway and molecular docking analyses, it may be concluded that frankincense and myrrh exert a negative effect on HCC through the regulation of angiogenesis and morphology, which are important pathological features of HCC. The progression of HCC depends on the local pathological environment, and hypoxia and inflammation are two key factors that affect this environment. This environment is also associated with angiogenesis, and both the process of local aberrant angiogenesis and the formation of vascular networks accelerate tumor growth, invasion and metastasis. The interaction of these factors further promotes the propagation of HCC[38,39]. The signaling pathways that control these processes are often dysregulated in the pathological progression of HCC. Therefore, these pathways have become an important source of targets for HCC therapy. As predicted by network pharmacology, frankincense and myrrh may display therapeutic effects on HCC mainly by enhancing the secretion of hypoxia-inducible factor HIF-1α, inflammatory factor TNF-α, *etc*. This enhanced secretion of these factors results in the regulation of EGFR and its mediation of the PI3K/Akt and

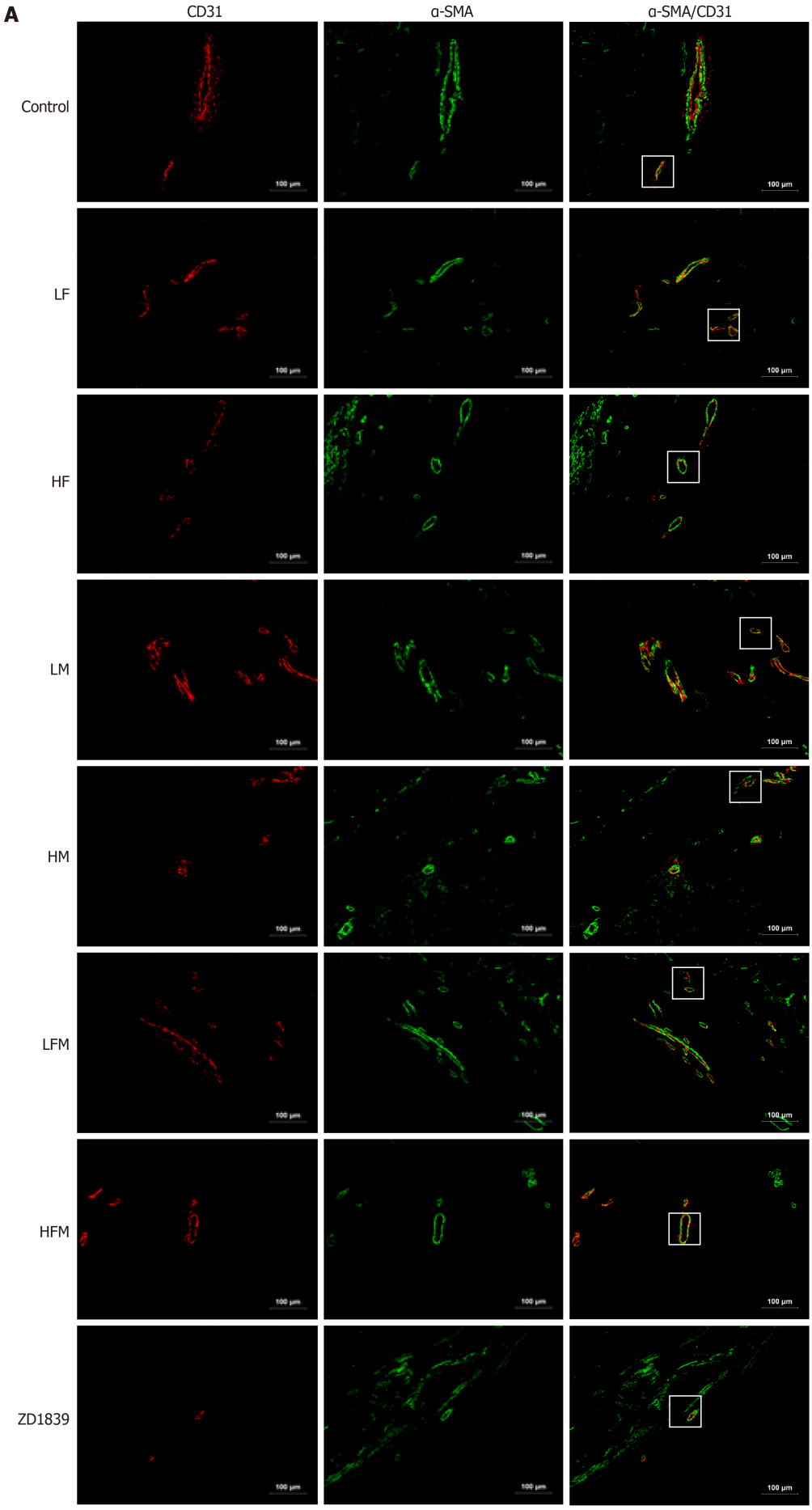
A
CD31
α-SMA
α-SMA/CD31
Control
LF
HF
LM
HM
LFM
HFM
ZD1839
100 μm

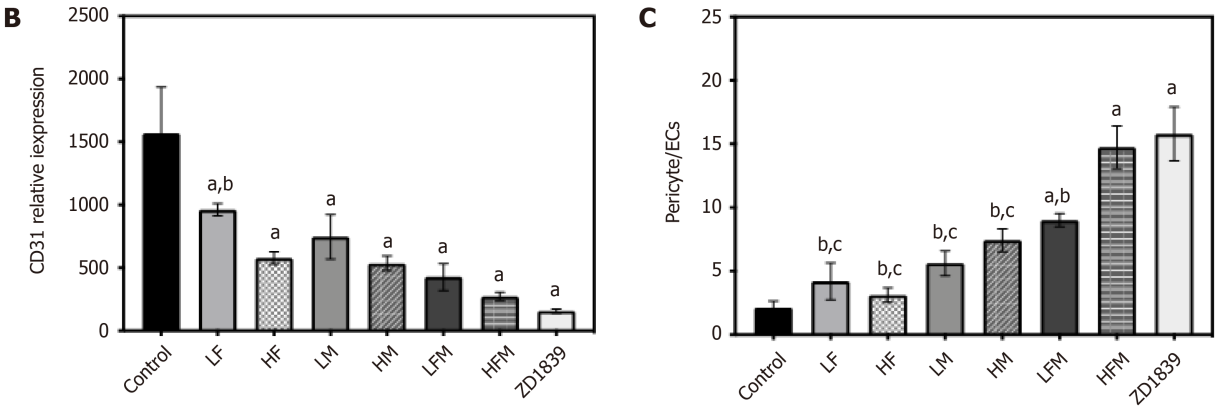


**Figure 5 The effect of frankincense and/or myrrh on CD31 and α-SMA (200×).** A: Immunofluorescence staining of the tumor was indicated by CD31 antibody (red) and α-SMA antibody (green); B: The relative expression of CD31; C: The expression of α-SMA/CD31. Scale bars: 100 μm. LF: Low dose of frankincense extract; HF: High dose of frankincense extract; LM: Low dose of myrrh extract; HM: High dose of myrrh extract; LFM: Low dose of frankincense + myrrh extracts; HFM: High dose of frankincense + myrrh extracts. Data represents the mean ± SE. $^{a}P < 0.05$ *vs* the model control; $^{b}P < 0.05$ *vs* ZD1839; $^{c}P < 0.05$ *vs* high dose of frankincense + myrrh extracts.

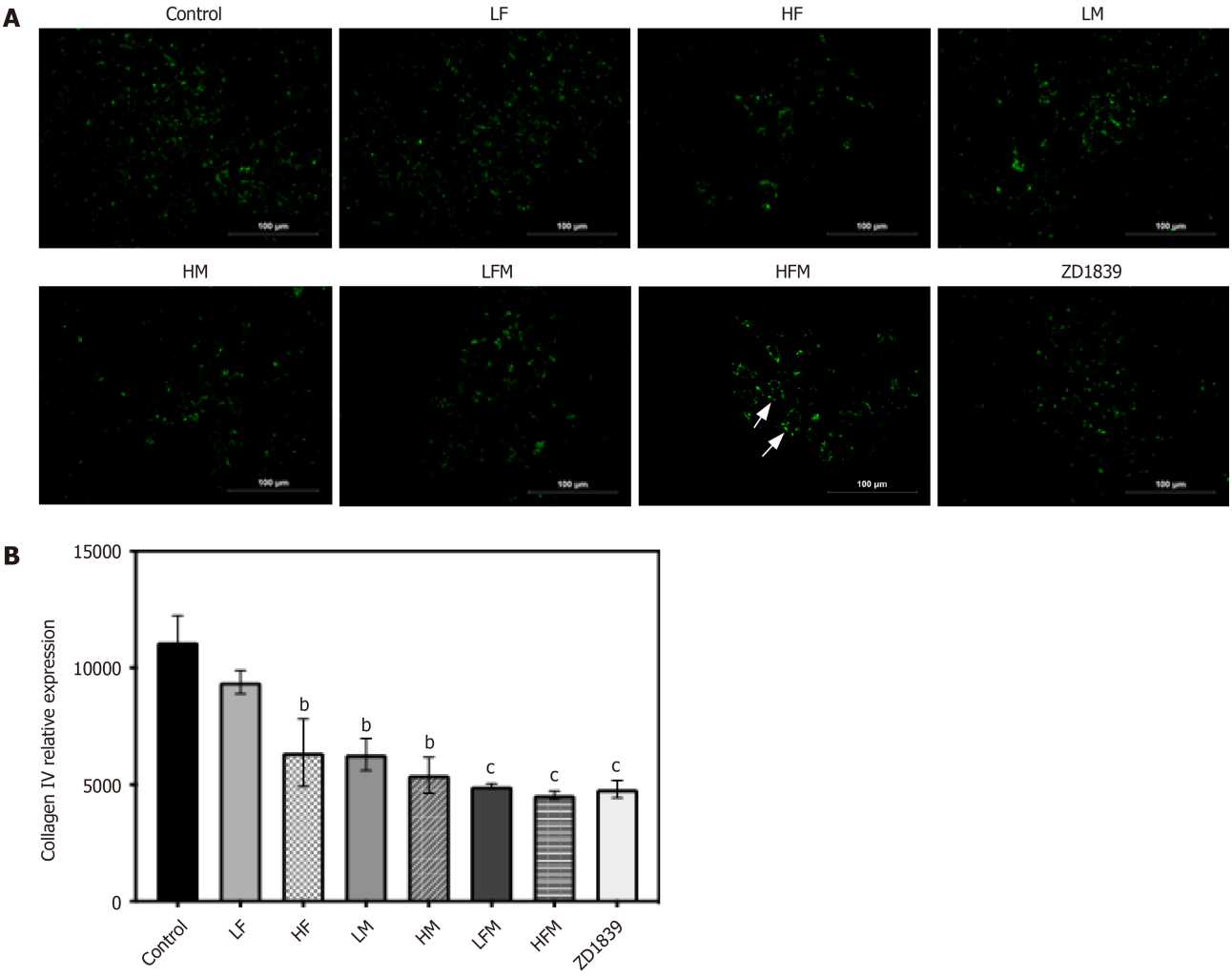


**Figure 6 The effect of frankincense and/or myrrh on collagen IV (400×).** A: Immunofluorescence staining of the tumor was indicated by collagen IV antibody (green); B: The relative expression of collagen IV. Scale bars: 100 μm. LF: Low dose of frankincense extract; HF: High dose of frankincense extract; LM: Low dose of myrrh extract; HM: High dose of myrrh extract; LFM: Low dose of frankincense + myrrh extracts; HFM: High dose of frankincense + myrrh extracts. Data represents the mean ± SE. Compared with the model control, $^{a}P < 0.05$, $^{b}P < 0.01$, $^{c}P < 0.001$.

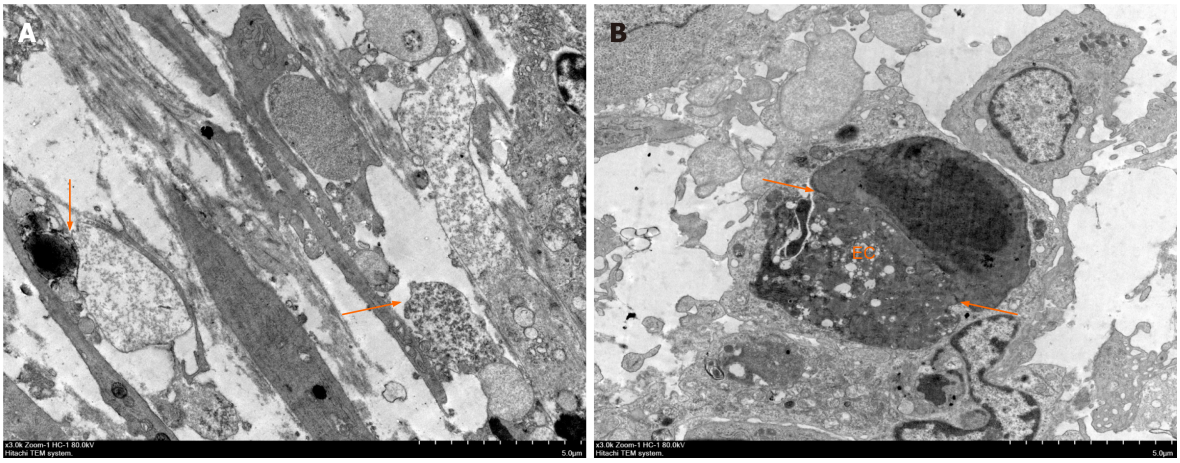


**Figure 7 The effect of frankincense and myrrh on tumor vascular cell ultrastructure (10000×).** A: The model control group; B: High dose of frankincense + myrrh extracts group; EC: Endothelial cells; P: Pericytes; →: Connection between cells.

MAPK signaling pathways. An additional effect is the modulated expression of tumor angiogenesis-related factors (such as VEGF and MMP-9), angiogenesis itself, and other abnormal morphological structures. To test this hypothesis, the efficacy of frankincense and/or myrrh extracts on nude mouse models with subcutaneously transplanted human liver cancer cells was investigated.

Persistent proangiogenic signaling in HCC diminishes the effect of the subsequent steps of normal vascular morphogenesis. This regulatory effect results in a dysfunctional vascular network with poor maturation and low stability characterized by EC hyperplasia, defective pericyte connections and basement membrane discontinuity and loosening. These effects contribute to disrupted vascular integrity and promote the growth of intravascular and metastatic cancer cells, exacerbating local hypoxia and inflammation and leading to the growth and spread of tumorous tissues. Restoring vascular connectivity and maintaining its integrity may be important strategies for the improvement of tumor vascularity and reduction in metastasis[40-42]. In this study, we found that treatment with frankincense and/or myrrh significantly reduced the volume and growth rate of tumors and improved the pathological morphology of tumors compared to the model control group. Frankincense and/or myrrh also lowered the expression levels of the EC-specific marker CD31 and reduced neointimal formation ($P < 0.05$) while upregulating pericyte coverage ($P < 0.05$), downregulating the expression of the basement membrane-specific marker collagen IV ($P < 0.01$) and increasing vascular maturation. In summary, these compounds improved EC connectivity, pericyte envelopment and basement membrane integrity, supporting the effects of frankincense and/or myrrh treatment on tumor growth and vascularity in a subcutaneous graft tumor model of HCC.

As HCC progresses, rapid tumor growth leads to the initiation of hypoxic responses and the onset of severe inflammation. This in turn results in increased angiogenesis with abnormal vessel morphology and the promotion of further tumor infiltration and metastasis[43]. HIF-1α, a recognized core mediator in the hypoxic environment of tumors, stimulates angiogenesis by acting in conjunction with TNF-α to drive VEGF production and upregulate MMP expression. HIF-1α has also been recognized as an independent novel marker in the prognosis of HCC. With activated HIF-1α, TNF-α is a major mediator of accelerated tumor inflammation[38,44,45]. It induces angiogenesis and enhances drug resistance by facilitating the establishment of a proinflammatory microenvironment around tumorous tissue. In this study, frankincense and/or myrrh was found to significantly reduce the production of both HIF-1α and TNF-α compared to the model control group ($P < 0.05$), demonstrating the effect of each extract on the respective markers associated with tumor hypoxia and inflammation.

VEGF is the most important factor in the stimulation of tumor angiogenesis. Often overexpressed in HCC, VEGF enhances vascular permeability and increases the expression of MMPs by protecting ECs from apoptosis. MMP-9 is a zinc-dependent protein hydrolase that degrades extracellular matrix components and increases capillary permeability, thereby promoting vascular leakage, EC dysregulation and tumor cell recirculation. It also significantly increases the levels of angiogenic cytokines while decreasing the levels of antiangiogenic factors, leading to the excessive proliferation and abnormal morphology of tumor vessels[31,46]. The results of this

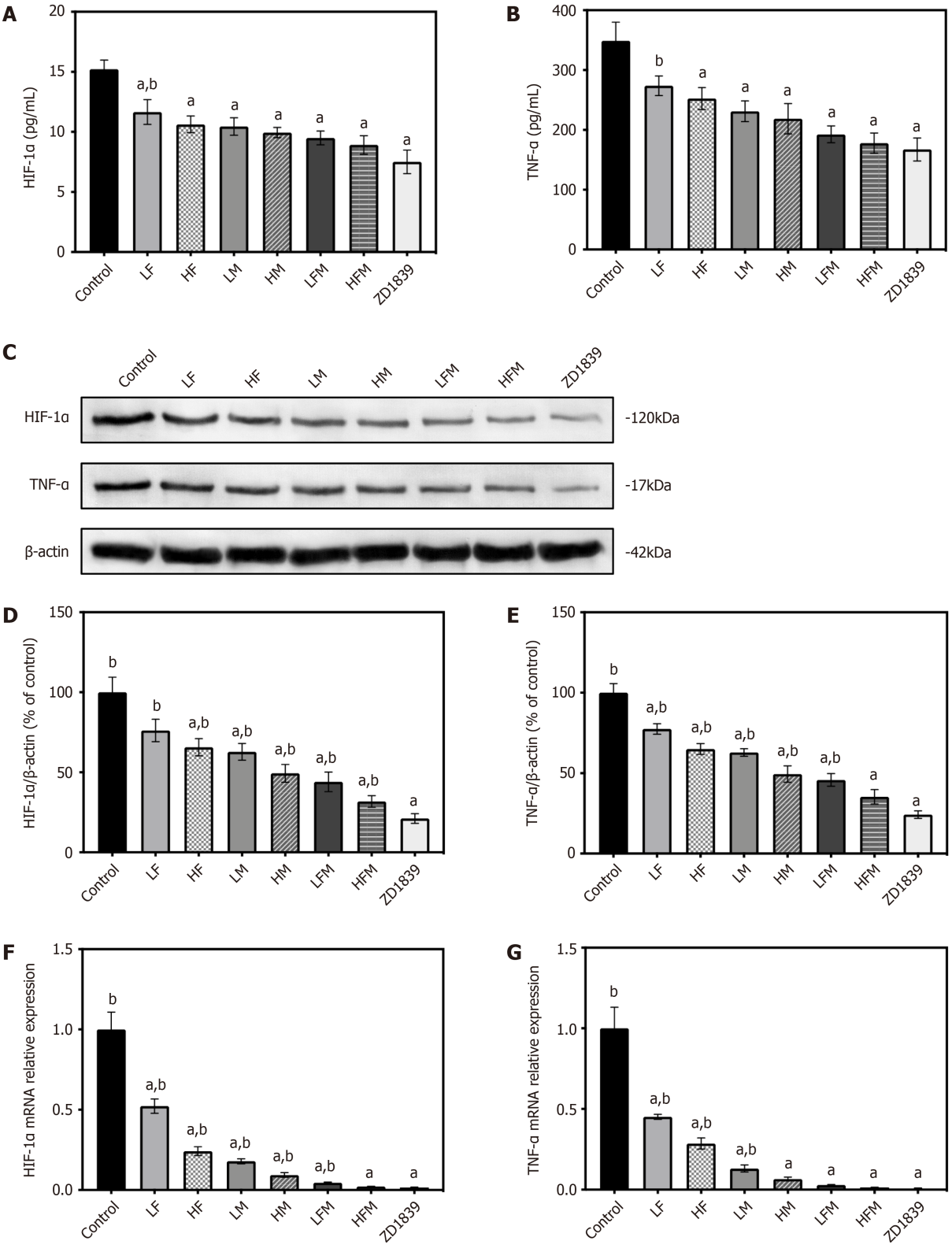


**Figure 8 The effect of frankincense and/or myrrh on HIF-1α and TNF-α.** A and B: The secretion of HIF-1α and TNF-α in tumor body was detected by enzyme-linked immunosorbent assay; C-E: The protein levels of HIF-1α and TNF-α in tumor body, the protein expression indicated with Western blot, and β-actin was used as internal control; F and G: The mRNA levels of HIF-1α and TNF-α in tumor body, the mRNA expression was analyzed using reverse transcription-polymerase chain reaction, with GAPDH was reference gene. LF: Low dose of frankincense extract; HF: High dose of frankincense extract; LM: Low dose of myrrh extract; HM: High dose of myrrh extract; LFM: Low dose of frankincense + myrrh extracts; HFM: High dose of frankincense + myrrh extracts. Data represents the mean ± SE. $^{a}P < 0.05$ *vs* the model control; $^{b}P < 0.05$ *vs* ZD1839.

study showed that frankincense plus myrrh significantly downregulated the mRNA and protein expression levels of both VEGF and MMP-9 in subcutaneous HCC xenograft tumors ($P < 0.05$), with performance that was superior to that of the control

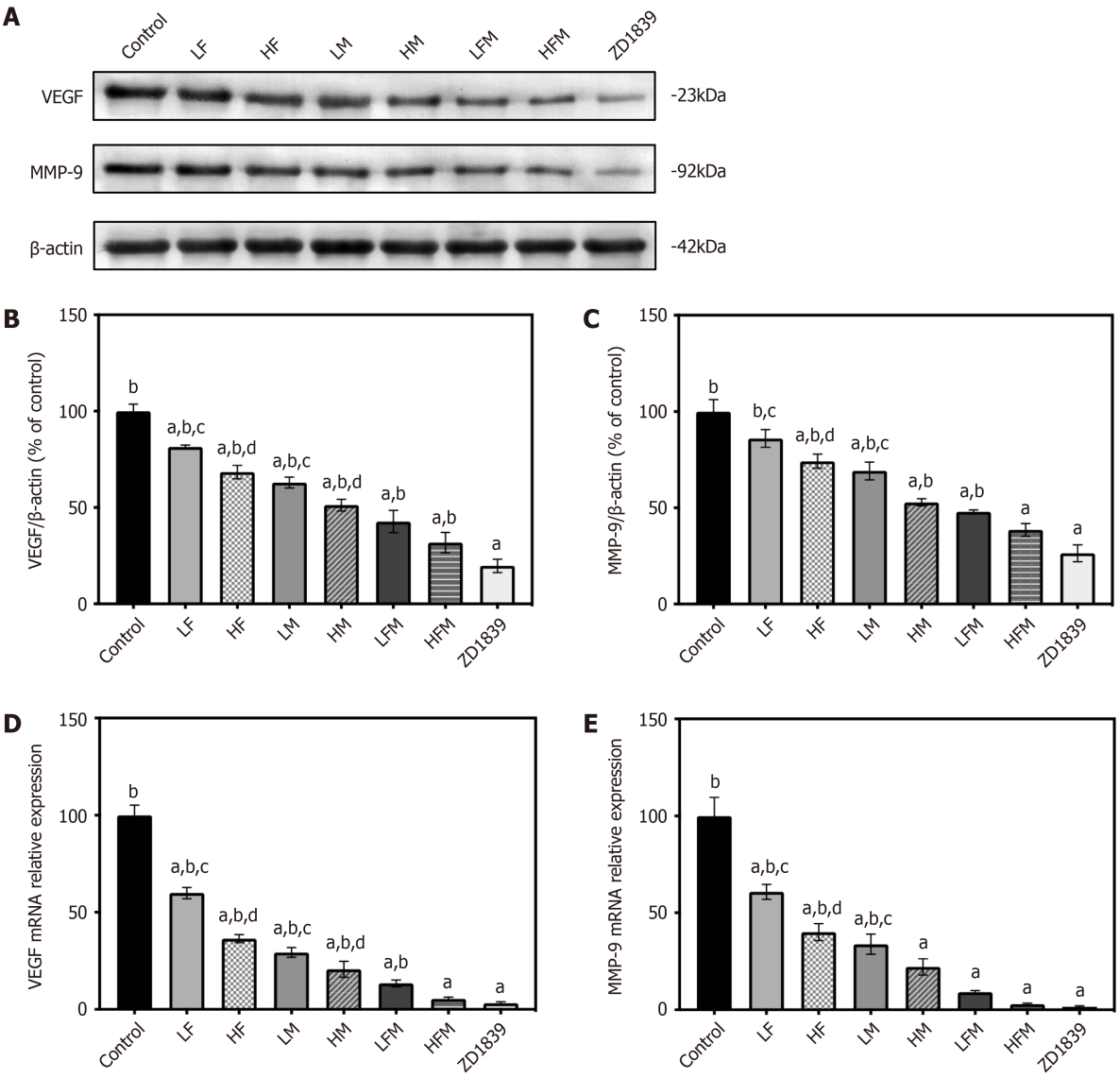


**Figure 9 The effect of frankincense and/or myrrh on VEGF and MMP-9.** A-C: The protein levels of VEGF and MMP-9 in tumor body, the protein expression indicated with Western blot, and β-actin was used as internal control; D and E: The mRNA levels of VEGF and MMP-9 in tumor body, the mRNA expression was analyzed using reverse transcription-polymerase chain reaction, with GAPDH was reference gene. LF: Low dose of frankincense extract; HF: High dose of frankincense extract; LM: Low dose of myrrh extract; HM: High dose of myrrh extract; LFM: Low dose of frankincense + myrrh extracts; HFM: High dose of frankincense + myrrh extracts. Data represents the mean ± SE. $^{a}P < 0.05$ *vs* the model control; $^{b}P < 0.05$ *vs* ZD1839; $^{c}P < 0.05$ *vs* low dose of frankincense + myrrh extracts; $^{d}P < 0.05$ *vs* high dose of frankincense + myrrh extracts.

group. This observation indicates that frankincense plus myrrh exerted an ameliorative effect on the abnormal morphology of tumor vessels, likely due to the reduced production of VEGF and MMP-9.

In the local pathological environment of HCC, the core factors of hypoxia and the inflammatory response, HIF-1α and TNF-α, function together to induce the expression of the angiogenesis-related factors VGEF and MMP-9, which in turn regulate the process of tumor vascularity, involving multiple signaling pathways. In this study, the regulation of these signaling pathways by frankincense and/or myrrh was examined and validated.

EGFR, which is also highly expressed in HCC, is a member of the tyrosine kinase receptor family and is recognized as a 'hub' for signaling convergence. Hypoxia and inflammation induce EGFR activation, leading to an increase in its intrinsic tyrosine kinase activity and the subsequent autophosphorylation and cross-phosphorylation of Tyr residues in its C-terminal tail. These activated receptors are recognized by effector molecules, activating the MAPK cascade of ERK, JNK and p38, as well as the PI3K/Akt pathway in the PKC mechanism. Thus, EGFR regulates several important processes in HCC, including tumor cell infiltration and angiogenesis. In this study, network pharmacology and molecular docking showed that components in the EGFR

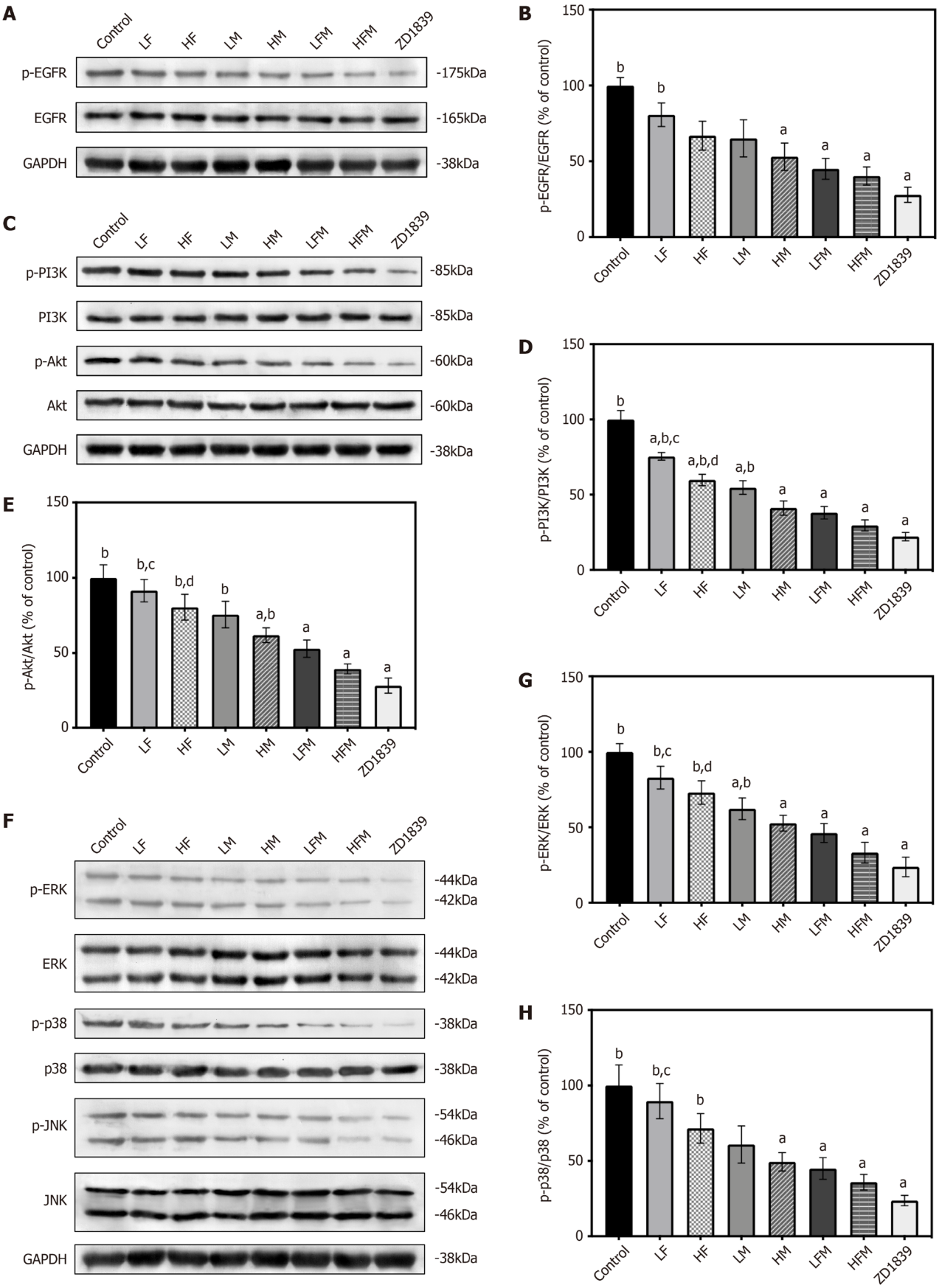
A
Control
LF
HF
LM
HM
LFM
HFM
ZD1839
p-EGFR
EGFR
GAPDH
-175kDa
-165kDa
-38kDa
B
p-EGFR/EGFR (% of control)
C
p-PI3K
PI3K
p-Akt
Akt
GAPDH
-85kDa
-85kDa
-60kDa
-60kDa
-38kDa
D
p-PI3K/PI3K (% of control)
E
p-Akt/Akt (% of control)
F
p-ERK
ERK
p-p38
p38
p-JNK
JNK
GAPDH
-44kDa
-42kDa
-44kDa
-42kDa
-38kDa
-38kDa
-54kDa
-46kDa
-54kDa
-46kDa
-38kDa
G
p-ERK/ERK (% of control)
H
p-p38/p38 (% of control)

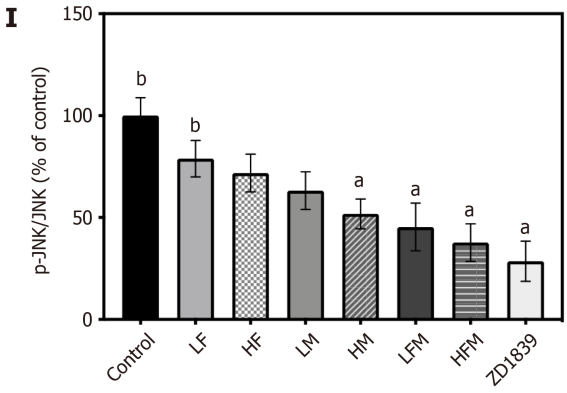


**Figure 10 The effect of frankincense and/or myrrh on EGFR, PI3K/Akt and MAPK (ERK, p38, JNK) pathway components.** A and B: The protein levels of EGFR, p-EGFR in tumor body; C-E: The protein levels of PI3K, p-PI3K, Akt, p-Akt in tumor body; F-I: The protein levels of EKR, p-ERK, p38, p-p38, JNK, p-JNK. The protein expression indicated with Western blot, and GAPDH was used as internal control. Data represents the mean ± SE. LF: Low dose of frankincense extract; HF: High dose of frankincense extract; LM: Low dose of myrrh extract; HM: High dose of myrrh extract; LFM: Low dose of frankincense + myrrh extracts; HFM: High dose of frankincense + myrrh extracts. Data represents the mean ± SE. $^{a}P < 0.05$ *vs* the model control; $^{b}P < 0.05$ *vs* ZD1839; $^{c}P < 0.05$ *vs* low dose of frankincense + myrrh extracts; $^{d}P < 0.05$ *vs* high dose of frankincense + myrrh extracts.

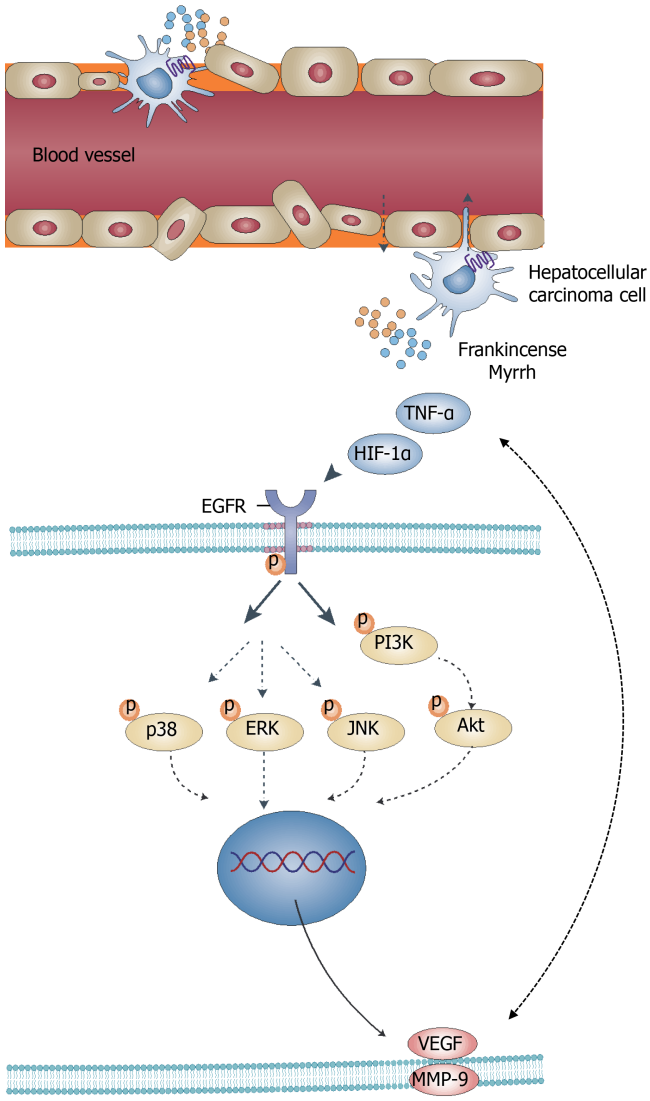


**Figure 11 Schematic of frankincense and myrrh as potential anti hepatocellular carcinoma therapeutic agents.**

signaling pathway are important targets and participants in the mechanism of action for frankincense and/or myrrh against HCC[47-49]. In contrast to the model control group, frankincense and/or myrrh was able to reduce EGFR phosphorylation in subcutaneously transplanted HCC tumors and inhibit EGFR activation, which verified the hypothesis concerning the effect of frankincense and myrrh on EGFR.

PI3K, a phosphatidylinositol monoenzyme that is activated *via* EGFR, phosphorylates and activates Akt. It has been demonstrated that the PI3K/Akt pathway in tumor cells increases the secretion of VEGF, upregulates the activity of matrix metalloproteinase MMPs and engages in crosstalk with other transduction pathways to induce structurally abnormal blood vessel formation. Together, these factors cause aberrations in tumor vessels and ischemia during vascular development, which play important roles in regulating tumor vasculature[33,50]. The results obtained in this work showed that an EGFR inhibitor can reduce the phosphorylation-induced activity of tumor PI3K/Akt. Furthermore, frankincense and/or myrrh effectively reduced the phosphorylation of PI3K and Akt in tumors, suggesting that frankincense and myrrh have an inhibitory effect on the PI3K/Akt signaling pathway.

MAPK belongs to the family of extracellular signal-regulated kinases, which also includes ERK, p38 and JNK; all three of these kinases are activated through phosphorylation, with ERK mediating EC differentiation in blood vessels and p38 and JNK downregulating the expression of the pericyte marker α-SMA. In tumors, the MAPK signaling pathway has a number of effects: Promoting the production of VEGF and MMP-9; increasing EC migration, tube formation and tumor angiogenesis; and acting synergistically with the PI3K/Akt pathway[34,50,51]. As detailed in this article, an EGFR inhibitor was found to downregulate the phosphorylation levels of ERK, p38 and JNK in subcutaneously transplanted HCC tumors. In the frankincense and myrrh treatment groups, the expression of p-ERK, p-p38 and p-JNK was lower extent than in the model control group. Thus, in the *in vivo* model, a possible conclusion is that the effect of frankincense and/or myrrh on tumor growth and vascularity may be partially achieved through the regulation of the MAPK signaling pathway.

## CONCLUSION

In general, this study predicted and proved that frankincense and/or myrrh targets tumor blood vessels to exert anti-HCC effects. The molecular mechanism may involve EGFR-mediated PI3K/Akt and MAPK signaling pathways. This study highlights the potential of frankincense and/or myrrh as anti-HCC drug candidates.

## ARTICLE HIGHLIGHTS

### *Research background*

Hepatocellular carcinoma (HCC) has the characteristics of high morbidity, high recurrence rate, high metastasis rate and high mortality rate, which seriously threaten human health. Therefore, it is necessary to find new treatment methods. In traditional Chinese medicine (TCM), the anti-HCC activity of the antitumor drug Xihuang Pill has attracted attention.

### *Research conclusions*

Frankincense and myrrh treatment targets tumor blood vessels to exert anti-HCC effects *via* EGFR-activated PI3K/Akt and MAPK signaling pathways.

### *Research results*

There are 35 active ingredients in frankincense and myrrh, with 151 key targets, and they may play roles in the treatment of HCC by regulating the hypoxia response and vascular-system-related pathological processes. Compared with the control group, after treatment with frankincense and/or myrrh, the volume of transplanted subcutaneously HCC tumors was significantly reduced, and the pathological morphology was weakened. The expression levels of CD31 and collagen IV were downregulated; the coverage of cells around blood vessels was upregulated; the connections between cells were tightened, and the shape of blood vessels was improved. In addition, frankincense and/or myrrh treatment downregulated the expression levels of HIF-1α, TNF-α, VEGF and MMP-9 and downregulated the phosphorylation activity of EGFR and downstream target PI3K/Akt and MAPK (ERK,

p38 and JNK) pathway-related proteins.

### Research methods

Bioinformatics analysis was used to predict the efficacy and possible mechanism of frankincense and myrrh in HCC and to screen core predictive targets. BALB/c nude mice were introduced *in vivo* to establish an HCC subcutaneous tumor model. The tumor volume and growth rate were evaluated, and histopathological examination was used to detect tumor growth, proliferation and pathological changes. Immunofluorescence and transmission electron microscopy were used to observe the expression of CD31, α-SMA and collagen IV and the morphology of vascular endothelial cells and pericytes. Enzyme-linked immunosorbent assay was utilized to detect the secretion of HIF-1α and TNF-α. Reverse transcription-quantitative polymerase chain reaction was applied to detect the expression levels of HIF-1α, TNF-α, VEGF and MMP-9. Western blot was adopted to detect EGFR and its mediated PI3K/Akt, MAPK (ERK, p38 and JNK) core signaling pathways and other key proteins as well as HIF-1α and TNF-α protein expression.

### Research objectives

To study the potential anti-HCC therapeutic targets and molecular mechanisms of frankincense and myrrh *in vivo*.

### Research motivation

The main components of Xihuang Pill, frankincense and myrrh, have shown anticancer activities in other biological systems. However, whether frankincense and/or myrrh can inhibit the occurrence of HCC is unclear, and the underlying molecular mechanism has not yet been determined.

### Research perspectives

The dual TCM compound frankincense and myrrh has the potential to become an anti-HCC drug candidate.

## ACKNOWLEDGEMENTS

The authors sincerely thank Dr. Lin-Tian Yuan of Perking University Hospital of Stomatology for his encouragement and support during this study. In addition, we are grateful to the young actor Jun Gong. His spirit of pursuing and persisting in his career has inspired our research.

## REFERENCES

1 **Gui Y**, Khan MGM, Bobbala D, Dubois C, Ramanathan S, Saucier C, Ilangumaran S. Attenuation of MET-mediated migration and invasion in hepatocellular carcinoma cells by SOCS1. *World J Gastroenterol* 2017; **23**: 6639-6649 [PMID: 29085209 DOI: 10.3748/wjg.v23.i36.6639]

2 **Kasprzak A**, Rogacki K, Adamek A, Sterzyńska K, Przybyszewska W, Seraszek-Jaros A, Helak-Łapaj C, Pyda P. Tissue expression of β-catenin and E- and N-cadherins in chronic hepatitis C and hepatocellular carcinoma. *Arch Med Sci* 2017; **13**: 1269-1280 [PMID: 29181057 DOI: 10.5114/aoms.2017.65272]

3 **McGlynn KA**, Petrick JL, El-Serag HB. Epidemiology of Hepatocellular Carcinoma. *Hepatology* 2021; **73** Suppl 1: 4-13 [PMID: 32319693 DOI: 10.1002/hep.31288]

4 **Martin JD**, Seano G, Jain RK. Normalizing Function of Tumor Vessels: Progress, Opportunities, and Challenges. *Annu Rev Physiol* 2019; **81**: 505-534 [PMID: 30742782 DOI: 10.1146/annurev-physiol-020518-114700]

5 **Viallard C**, Larrivée B. Tumor angiogenesis and vascular normalization: alternative therapeutic targets. *Angiogenesis* 2017; **20**: 409-426 [PMID: 28660302 DOI: 10.1007/s10456-017-9562-9]

6 **Martin JD**, Fukumura D, Duda DG, Boucher Y, Jain RK. Reengineering the Tumor Microenvironment to Alleviate Hypoxia and Overcome Cancer Heterogeneity. *Cold Spring Harb Perspect Med* 2016; **6** [PMID: 27663981 DOI: 10.1101/cshperspect.a027094]

7 **Jain RK**. Normalization of tumor vasculature: an emerging concept in antiangiogenic therapy. *Science* 2005; **307**: 58-62 [PMID: 15637262 DOI: 10.1126/science.1104819]

8 **Wattenberg MM**, Damjanov N, Kaplan DE. Utility of bevacizumab in advanced hepatocellular carcinoma: A veterans affairs experience. *Cancer Med* 2019; **8**: 1442-1446 [PMID: 30790466 DOI: 10.1002/cam4.2015]

9 **Roderburg C**, Özdirik B, Wree A, Demir M, Tacke F. Systemic treatment of hepatocellular

carcinoma: from sorafenib to combination therapies. *Hepat Oncol* 2020; **7**: HEP20 [PMID: 32647565 DOI: 10.2217/hep-2020-0004]

10 **Chuai Y**, Rizzuto I, Zhang X, Li Y, Dai G, Otter SJ, Bharathan R, Stewart A, Wang A. Vascular endothelial growth factor (VEGF) targeting therapy for persistent, recurrent, or metastatic cervical cancer. *Cochrane Database Syst Rev* 2021; **3**: CD013348 [PMID: 33661538 DOI: 10.1002/14651858.CD013348.pub2]

11 **Simon T**, Gagliano T, Giamas G. Direct Effects of Anti-Angiogenic Therapies on Tumor Cells: VEGF Signaling. *Trends Mol Med* 2017; **23**: 282-292 [PMID: 28162910 DOI: 10.1016/j.molmed.2017.01.002]

12 **Raybould AL**, Sanoff H. Combination Antiangiogenic and Immunotherapy for Advanced Hepatocellular Carcinoma: Evidence to Date. *J Hepatocell Carcinoma* 2020; **7**: 133-142 [PMID: 32984090 DOI: 10.2147/JHC.S224938]

13 **Zhang W**, Sun HC, Wang WQ, Zhang QB, Zhuang PY, Xiong YQ, Zhu XD, Xu HX, Kong LQ, Wu WZ, Wang L, Song TQ, Li Q, Tang ZY. Sorafenib down-regulates expression of HTATIP2 to promote invasiveness and metastasis of orthotopic hepatocellular carcinoma tumors in mice. *Gastroenterology* 2012; **143**: 1641-1649.e5 [PMID: 22922424 DOI: 10.1053/j.gastro.2012.08.032]

14 **Yang X**, Wu XZ. Main Anti-tumor Angiogenesis Agents Isolated From Chinese Herbal Medicines. *Mini Rev Med Chem* 2015; **15**: 1011-1023 [PMID: 26156539 DOI: 10.2174/1389557515112150731113242]

15 **Khan MA**, Ali R, Parveen R, Najmi AK, Ahmad S. Pharmacological evidences for cytotoxic and antitumor properties of Boswellic acids from Boswellia serrata. *J Ethnopharmacol* 2016; **191**: 315-323 [PMID: 27346540 DOI: 10.1016/j.jep.2016.06.053]

16 **Ahmad MA**, Mujeeb M, Akhtar M, Khushtar M, Arif M, Haque MR. Guggulipid: A Promising Multi-Purpose Herbal Medicinal Agent. *Drug Res (Stuttg)* 2020; **70**: 123-130 [PMID: 32110820 DOI: 10.1055/a-1115-4669]

17 **Zhao X**, Hao J, Chen S. Network Pharmacology-Based Strategy for Predicting Therapy Targets of Traditional Chinese Medicine Xihuang Pill on Liver Cancer. *Evid Based Complement Alternat Med* 2020; **2020**: 6076572 [PMID: 32256653 DOI: 10.1155/2020/6076572]

18 **Yadav VR**, Prasad S, Sung B, Gelovani JG, Guha S, Krishnan S, Aggarwal BB. Boswellic acid inhibits growth and metastasis of human colorectal cancer in orthotopic mouse model by downregulating inflammatory, proliferative, invasive and angiogenic biomarkers. *Int J Cancer* 2012; **130**: 2176-2184 [PMID: 21702037 DOI: 10.1002/ijc.26251]

19 **Sun M**, Hua J, Liu G, Huang P, Liu N, He X. Myrrh induces the apoptosis and inhibits the proliferation and migration of gastric cancer cells through down-regulating cyclooxygenase-2 expression. *Biosci Rep* 2020; **40** [PMID: 32364228 DOI: 10.1042/bsr20192372]

20 **Gao R**, Miao X, Sun C, Su S, Zhu Y, Qian D, Ouyang Z, Duan J. Frankincense and myrrh and their bioactive compounds ameliorate the multiple myeloma through regulation of metabolome profiling and JAK/STAT signaling pathway based on U266 cells. *BMC Complement Med Ther* 2020; **20**: 96 [PMID: 32293402 DOI: 10.1186/s12906-020-2874-0]

21 **Chen Y**, Zhou C, Ge Z, Liu Y, Feng W, Li S, Chen G, Wei T. Composition and potential anticancer activities of essential oils obtained from myrrh and frankincense. *Oncol Lett* 2013; **6**: 1140-1146 [PMID: 24137478 DOI: 10.3892/ol.2013.1520]

22 **Guo W**, Huang J, Wang N, Tan HY, Cheung F, Chen F, Feng Y. Integrating Network Pharmacology and Pharmacological Evaluation for Deciphering the Action Mechanism of Herbal Formula Zuojin Pill in Suppressing Hepatocellular Carcinoma. *Front Pharmacol* 2019; **10**: 1185 [PMID: 31649545 DOI: 10.3389/fphar.2019.01185]

23 **Dashti S**, Taheri M, Ghafouri-Fard S. An in-silico method leads to recognition of hub genes and crucial pathways in survival of patients with breast cancer. *Sci Rep* 2020; **10**: 18770 [PMID: 33128008 DOI: 10.1038/s41598-020-76024-2]

24 **Ruan X**, Du P, Zhao K, Huang J, Xia H, Dai D, Huang S, Cui X, Liu L, Zhang J. Mechanism of Dayuanyin in the treatment of coronavirus disease 2019 based on network pharmacology and molecular docking. *Chin Med* 2020; **15**: 62 [PMID: 32536965 DOI: 10.1186/s13020-020-00346-6]

25 **Tian S**, Liao L, Zhou Q, Huang X, Zheng P, Guo Y, Deng T, Tian X. Curcumin inhibits the growth of liver cancer by impairing myeloid-derived suppressor cells in murine tumor tissues. *Oncol Lett* 2021; **21**: 286 [PMID: 33732362 DOI: 10.3892/ol.2021.12547]

26 **Dhar D**, Antonucci L, Nakagawa H, Kim JY, Glitzner E, Caruso S, Shalapour S, Yang L, Valasek MA, Lee S, Minnich K, Seki E, Tuckermann J, Sibilia M, Zucman-Rossi J, Karin M. Liver Cancer Initiation Requires p53 Inhibition by CD44-Enhanced Growth Factor Signaling. *Cancer Cell* 2018; **33**: 1061-1077.e6 [PMID: 29894692 DOI: 10.1016/j.ccell.2018.05.003]

27 **Krishna Priya S**, Nagare RP, Sneha VS, Sidhanth C, Bindhya S, Manasa P, Ganesan TS. Tumour angiogenesis-Origin of blood vessels. *Int J Cancer* 2016; **139**: 729-735 [PMID: 26934471 DOI: 10.1002/ijc.30067]

28 **Marchand M**, Monnot C, Muller L, Germain S. Extracellular matrix scaffolding in angiogenesis and capillary homeostasis. *Semin Cell Dev Biol* 2019; **89**: 147-156 [PMID: 30165150 DOI: 10.1016/j.semcdb.2018.08.007]

29 **Wen Y**, Zhou X, Lu M, He M, Tian Y, Liu L, Wang M, Tan W, Deng Y, Yang X, Mayer MP, Zou F, Chen X. Bclaf1 promotes angiogenesis by regulating HIF-1α transcription in hepatocellular carcinoma. *Oncogene* 2019; **38**: 1845-1859 [PMID: 30367150 DOI: 10.1038/s41388-018-0552-1]

30 **Jin F**, Zheng X, Yang Y, Yao G, Ye L, Doeppner TR, Hermann DM, Wang H, Dai Y. Impairment of

hypoxia-induced angiogenesis by LDL involves a HIF-centered signaling network linking inflammatory TNFα and angiogenic VEGF. *Aging (Albany NY)* 2019; **11**: 328-349 [PMID: 30659163 DOI: 10.18632/aging.101726]

31 **Xu Q**, Gu J, Lv Y, Yuan J, Yang N, Chen J, Wang C, Hou X, Jia X, Feng L, Yin G. Angiogenesis for tumor vascular normalization of Endostar on hepatoma 22 tumor-bearing mice is involved in the immune response. *Oncol Lett* 2018; **15**: 3437-3446 [PMID: 29467868 DOI: 10.3892/ol.2018.7734]

32 **Yu X**, Li W, Deng Q, You S, Liu H, Peng S, Liu X, Lu J, Luo X, Yang L, Tang M, Weng X, Yi W, Liu W, Wu S, Ding Z, Feng T, Zhou J, Fan J, Bode AM, Dong Z, Liu J, Cao Y. Neoalbaconol inhibits angiogenesis and tumor growth by suppressing EGFR-mediated VEGF production. *Mol Carcinog* 2017; **56**: 1414-1426 [PMID: 27996164 DOI: 10.1002/mc.22602]

33 **Karar J**, Maity A. PI3K/AKT/mTOR Pathway in Angiogenesis. *Front Mol Neurosci* 2011; **4**: 51 [PMID: 22144946 DOI: 10.3389/fnmol.2011.00051]

34 **Tsai HC**, Cheng SP, Han CK, Huang YL, Wang SW, Lee JJ, Lai CT, Fong YC, Tang CH. Resistin enhances angiogenesis in osteosarcoma *via* the MAPK signaling pathway. *Aging (Albany NY)* 2019; **11**: 9767-9777 [PMID: 31719210 DOI: 10.18632/aging.102423]

35 **Roy NK**, Parama D, Banik K, Bordoloi D, Devi AK, Thakur KK, Padmavathi G, Shakibaei M, Fan L, Sethi G, Kunnumakkara AB. An Update on Pharmacological Potential of Boswellic Acids against Chronic Diseases. *Int J Mol Sci* 2019; **20** [PMID: 31443458 DOI: 10.3390/ijms20174101]

36 **Kangsamaksin T**, Chaithongyot S, Wootthichairangsan C, Hanchaina R, Tangshewinsirikul C, Svasti J. Lupeol and stigmasterol suppress tumor angiogenesis and inhibit cholangiocarcinoma growth in mice *via* downregulation of tumor necrosis factor-α. *PLoS One* 2017; **12**: e0189628 [PMID: 29232409 DOI: 10.1371/journal.pone.0189628]

37 **Liao H**, Zhu D, Bai M, Chen H, Yan S, Yu J, Zhu H, Zheng W, Fan G. Stigmasterol sensitizes endometrial cancer cells to chemotherapy by repressing Nrf2 signal pathway. *Cancer Cell Int* 2020; **20**: 480 [PMID: 33041661 DOI: 10.1186/s12935-020-01470-x]

38 **Zhang J**, Zhang Q, Lou Y, Fu Q, Chen Q, Wei T, Yang J, Tang J, Wang J, Chen Y, Zhang X, Zhang J, Bai X, Liang T. Hypoxia-inducible factor-1α/interleukin-1β signaling enhances hepatoma epithelial-mesenchymal transition through macrophages in a hypoxic-inflammatory microenvironment. *Hepatology* 2018; **67**: 1872-1889 [PMID: 29171040 DOI: 10.1002/hep.29681]

39 **Dai CX**, Gao Q, Qiu SJ, Ju MJ, Cai MY, Xu YF, Zhou J, Zhang BH, Fan J. Hypoxia-inducible factor-1 alpha, in association with inflammation, angiogenesis and MYC, is a critical prognostic factor in patients with HCC after surgery. *BMC Cancer* 2009; **9**: 418 [PMID: 19948069 DOI: 10.1186/1471-2407-9-418]

40 **Meng J**, Liu Y, Han J, Tan Q, Chen S, Qiao K, Zhou H, Sun T, Yang C. Hsp90β promoted endothelial cell-dependent tumor angiogenesis in hepatocellular carcinoma. *Mol Cancer* 2017; **16**: 72 [PMID: 28359326 DOI: 10.1186/s12943-017-0640-9]

41 **De Palma M**, Biziato D, Petrova TV. Microenvironmental regulation of tumour angiogenesis. *Nat Rev Cancer* 2017; **17**: 457-474 [PMID: 28706266 DOI: 10.1038/nrc.2017.51]

42 **Agrawal V**, Maharjan S, Kim K, Kim NJ, Son J, Lee K, Choi HJ, Rho SS, Ahn S, Won MH, Ha SJ, Koh GY, Kim YM, Suh YG, Kwon YG. Direct endothelial junction restoration results in significant tumor vascular normalization and metastasis inhibition in mice. *Oncotarget* 2014; **5**: 2761-2777 [PMID: 24811731 DOI: 10.18632/oncotarget.1942]

43 **Myung SJ**, Yoon JH. [Hypoxia in hepatocellular carcinoma]. *Korean J Hepatol* 2007; **13**: 9-19 [PMID: 17380070]

44 **Wang M**, Zhao X, Zhu D, Liu T, Liang X, Liu F, Zhang Y, Dong X, Sun B. HIF-1α promoted vasculogenic mimicry formation in hepatocellular carcinoma through LOXL2 up-regulation in hypoxic tumor microenvironment. *J Exp Clin Cancer Res* 2017; **36**: 60 [PMID: 28449718 DOI: 10.1186/s13046-017-0533-1]

45 **Luo D**, Wang Z, Wu J, Jiang C. The role of hypoxia inducible factor-1 in hepatocellular carcinoma. *Biomed Res Int* 2014; **2014**: 409272 [PMID: 25101278 DOI: 10.1155/2014/409272]

46 **Ren F**, Wu K, Yang Y, Wang Y, Li J. Dandelion Polysaccharide Exerts Anti-Angiogenesis Effect on Hepatocellular Carcinoma by Regulating VEGF/HIF-1α Expression. *Front Pharmacol* 2020; **11**: 460 [PMID: 32322211 DOI: 10.3389/fphar.2020.00460]

47 **Hu H**, Miao XK, Li JY, Zhang XW, Xu JJ, Zhang JY, Zhou TX, Hu MN, Yang WL, Mou LY. YC-1 potentiates the antitumor activity of gefitinib by inhibiting HIF-1α and promoting the endocytic trafficking and degradation of EGFR in gefitinib-resistant non-small-cell lung cancer cells. *Eur J Pharmacol* 2020; **874**: 172961 [PMID: 32044322 DOI: 10.1016/j.ejphar.2020.172961]

48 **Berasain C**, Nicou A, Garcia-Irigoyen O, Latasa MU, Urtasun R, Elizalde M, Salis F, Perugorría MJ, Prieto J, Recio JA, Corrales FJ, Avila MA. Epidermal growth factor receptor signaling in hepatocellular carcinoma: inflammatory activation and a new intracellular regulatory mechanism. *Dig Dis* 2012; **30**: 524-531 [PMID: 23108309 DOI: 10.1159/000341705]

49 **Berasain C**, Ujue Latasa M, Urtasun R, Goñi S, Elizalde M, Garcia-Irigoyen O, Azcona M, Prieto J, Avila MA. Epidermal Growth Factor Receptor (EGFR) Crosstalks in Liver Cancer. *Cancers (Basel)* 2011; **3**: 2444-2461 [PMID: 24212818 DOI: 10.3390/cancers3022444]

50 **Adya R**, Tan BK, Punn A, Chen J, Randeva HS. Visfatin induces human endothelial VEGF and MMP-2/9 production *via* MAPK and PI3K/Akt signalling pathways: novel insights into visfatin-induced angiogenesis. *Cardiovasc Res* 2008; **78**: 356-365 [PMID: 18093986 DOI: 10.1093/cvr/cvm111]

51 **Harding A**, Cortez-Toledo E, Magner NL, Beegle JR, Coleal-Bergum DP, Hao D, Wang A, Nolta

JA, Zhou P. Highly Efficient Differentiation of Endothelial Cells from Pluripotent Stem Cells Requires the MAPK and the PI3K Pathways. *Stem Cells* 2017; **35**: 909-919 [PMID: 28248004 DOI: 10.1002/stem.2577]

Published by **Baishideng Publishing Group Inc**
7041 Koll Center Parkway, Suite 160, Pleasanton, CA 94566, USA
**Telephone:** +1-925-3991568
**E-mail:** bpgoffice@wjgnet.com
**Help Desk:** https://www.f6publishing.com/helpdesk
https://www.wjgnet.com